

POLITECNICO DI TORINO

Master of Science in Biomedical Engineering

Master's Degree Thesis

**Effect of region-specific functional roles
within lower limb muscles on muscle synergies extraction**



Supervisors:

Marco Gazzoni

Taian Martins Vieira

Candidate:

Lorenzo Cavagnino

December 2019

To my parents Massimo and Monica,
who have always made me a truly happy son.

To my sister Ilaria,
who is always there to cover my back when I mess up.

To my love Elisa,
who has lived every moment of this journey with me and will live many more.

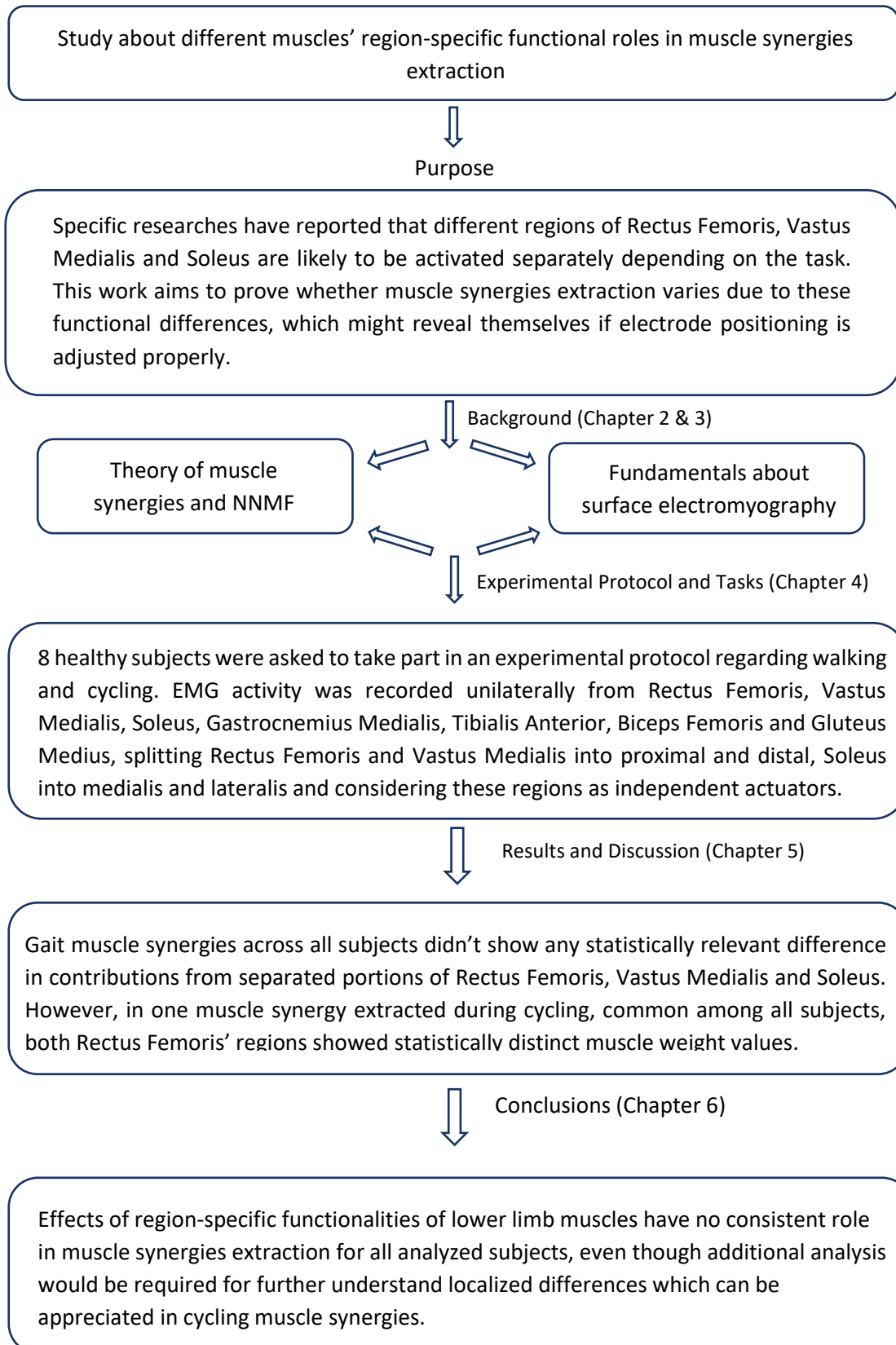
To my tennis coach and friend Stefano,
who has taught me how to be a better player and person.

Index

Index.....	3
Summary	5
Abstract.....	6
1. Introduction	7
2. EMG signal and electromyography	9
2.1 Generation of the EMG signal.....	9
2.2 Introduction to surface EMG and comparison with iEMG	11
2.3 sEMG detection configurations and spatial filters.....	14
3. Muscle synergies extraction.....	17
3.1 Concept of muscle synergies.....	17
3.2 Theory of muscle synergies: time-dependent synergies and synchronous synergies.	17
3.3 Muscle synergies extraction algorithm: NNMF.....	20
3.4 Muscle synergies extraction during gait and bike: previous studies shown in literature	23
4. Materials and methods	26
4.1 Subjects	26
4.2 Experimental protocol.....	26
4.3 Materials and skin preparation	26
4.4 Selected muscles	29
4.5 Electrodes positioning.....	32
4.6 Chosen parameters for EMG and biomechanical signals elaboration and muscle synergies extraction	39
4.7 Post-processing and indicators for synergies comparison.....	42
5. Results.....	46
5.1 Envelopes from Rectus Femoris during Gait: preliminary comparison with Watanabe et al. ^[35] study.....	46
5.2 Muscle synergies extraction results - Gait	49
5.3 Envelopes from Rectus Femoris in Cycling.....	55
5.4 Muscle synergies extraction results - Cycling	57
5.5 Results discussion.....	63
6. Conclusions	65
Appendix A - anatomical pictures for each muscle with relative electrode positioning	66

Appendix B - Informed Consent..... 69
Appendix C – Electrodes and skin preparation 71
Bibliography 73
Acknowledgements..... 77

Summary



Abstract

Muscle synergies are a widely recognized model of how the central nervous system overcomes the redundancy of the musculoskeletal system. Usually they are studied from surface EMG sampling one EMG signal from each muscle involved in the considered movement. However, specific studies showed that separated regions of some lower limb muscles (rectus femoris and vastus medialis for instance) may be excited independently. If, during a given motor task, different regions of the same muscle are elicited at different instants, it is then possible that a single muscle participates in different synergies.

In this study, the main focus is extracting muscle synergies considering different regions of selected lower-limb muscles as totally distinct actuators. Multichannel sEMG detection has been used to simulate the sampling of these muscles' activity from different locations and with different pick-up volumes and to check if different portions of the same muscle are involved in different synergies.

Eight healthy subjects participated in the study. EMG signals were detected from 8 muscles (Rectus Femoris, Vast Medialis, Gluteus Medius, Biceps Femoris, Tibialis Anterior, Gastrocnemius Medialis and Soleus) during over ground gait at self-selected speed, gait on treadmill at pre-selected speed and cycling on a stationary bike at a pre-chosen pace and fixed resistance. Multiple electrodes were positioned on Rectus Femoris, Vastus Medialis and Soleus with the specific focus of detecting differences in the regional EMG activation, distinguishing proximal and lateral portions for the first two, medialis and lateralis for Soleus.

Muscle synergies extraction was performed with Matlab 2017a NMF (Non Negative Matrix Factorization) routine. No statistical evidence of clear differences in synergies weight values were found in gait analysis, since Rectus Femoris, Medial Gastrocnemius and Soleus Lateralis and Medialis do not actually play a significant role as distinguished muscle portions rather than a whole. However, in cycling analysis one muscle synergy, common to all subjects, highlighted Rectus Femoris' internal differences through statistically distinguished muscle weights. Further analysis is encouraged to fully understand this and other localised variations reported in a few subjects.

1. Introduction

In modern research environments related to clinics, robotics, rehabilitation and sport science, muscle synergies extraction is rapidly becoming a widespread tool to monitor muscle activity and interpret central nervous system's mechanisms to control our muscles during a task. Simplifying movement production is their main function and in the extraction process all analysed muscles are considered as independent actuators which combine themselves with precise timing during a specific task. However, specific studies ^{[1][2][3]} have shown that certain muscles' portions seem to be more involved in certain task phases than others and vice versa, since they have different functional roles. This has led to hypothesize that muscle synergies might be influenced by these peculiar traits and specifically that considering some muscles' regions as independent muscles could highlight their region-specific functional differences even in synergies extraction outcomes.

Since the main focus is on muscles whose regions show different levels of activation depending on the required function, searching literature was a key aspect to choose analysed muscles wisely. Barroso et. al., 2014 ^[20] was set as the reference article for muscle synergies comparison, since they investigated muscle synergies for both walking and cycling in healthy subjects, even though comparable results concerning gait muscle synergies have also been obtained by Clark et al. ^[25] and Olivera et al. ^[18].

It's documented in multiple works that most lower limb muscles (such as rectus femoris, gastrocnemius, hamstrings, etc.) can't be said to have a local region where their innervation zone is delimited, in fact it is quite the opposite: their innervation zone is usually scattered or distributed in complex configurations ^[21]. Therefore, due to their fibers' organization pattern and pinnation, lower limb muscles require great attention to place all required electrodes correctly.

Since muscle synergies extraction during walking and cycling is now commonly investigated in literature, this study is carried out to investigate them with a pronounced focus on finding any specific behaviour induced by some muscles' region-specific functionalities. This study

presents itself as an evaluation of the effects of internal functional differences in lower limb muscles on muscle synergies extraction. In particular, synergies' muscle weights are the most important variable to consider in order to spot any evident difference in the outcome of synergies extraction, since each of them is a quantitative measure of the involvement of a certain muscle (or portion of a muscle) in a synergy. Some differences in the activation profiles are possible too, even though they might be difficult to spot due to EMG variability.

Muscle synergies extraction was performed on Matlab 2017a[®] with Matlab[®] NNMF (non negative matrix factorization) routine while pre, postprocessing and results visualization were executed with customized Matlab[®] scripts. Extracted muscle synergies are compared first with those found in other studies to check algorithm stability and effectiveness; then, any difference between same muscle' regions shown in the extraction outcome is evaluated and finally its repeatability among all analysed subjects is checked.

2. EMG signal and electromyography

2.1 Generation of the EMG signal

A standard technique to study behaviours and functions of skeletal muscles is electromyography, which is analysing how muscles generate bioelectrical signals.

A brief description of the human neuromuscular system is needed to understand how it creates muscular potentials (fig.2.1.1 and fig.2.1.2): our muscles are made up of fibers and different groups of fibers are associated to a specific motoneuron, which selectively controls them by receiving impulses from the central neuronal drive and managing activations of its own associated fibers accordingly. This is possible thanks to acetylcholine, a neurotransmitter which is released by motoneurons: it binds to acetylcholine specific receptors and causes the opening of ion channels. Sodium ions are then able to flow into muscle cells, creating a depolarization across their membranes and triggering a muscle action potential, which spreads through each activated fiber. The connection point between a muscle fiber and its motoneuron of reference is a specialized synapse called neuromuscular junction. All neuromuscular junctions together outline a region called innervation zone (fig. 2.1.3), from which twitches start to spread along the fibers. Once they reach the tendon, located at the terminal end of the muscle, all potentials die out.

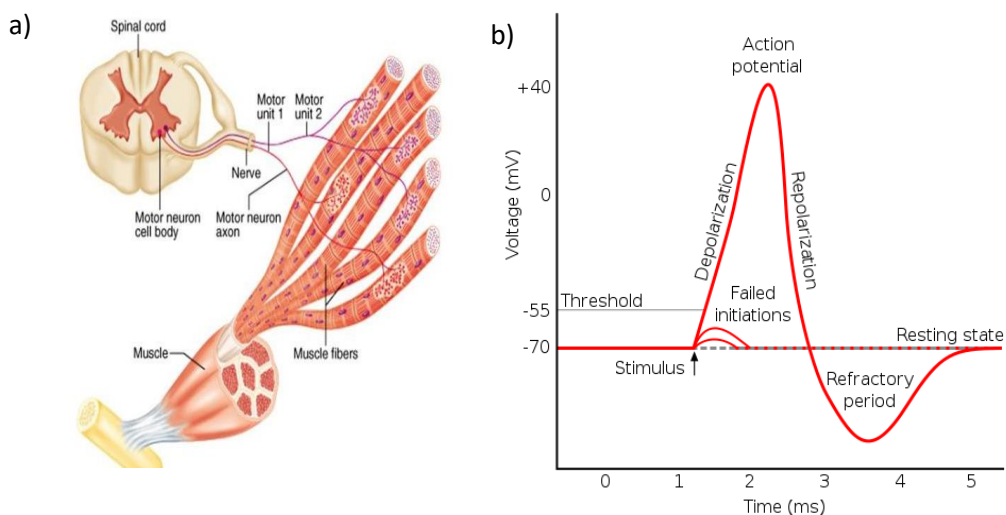


Figure 2.1.1: a) a stimulus is sent by the central nervous system to a spinal drive which redirects the electrical impulse to muscle fibers thanks to their associated motoneurons; b) shape of a typical muscle cell's action potential: a first ionic uptake triggers the depolarization after a certain quantity of acetylcholine is reached and then a progressive repolarization occurs. At last, the muscle cell enters its refractory period.

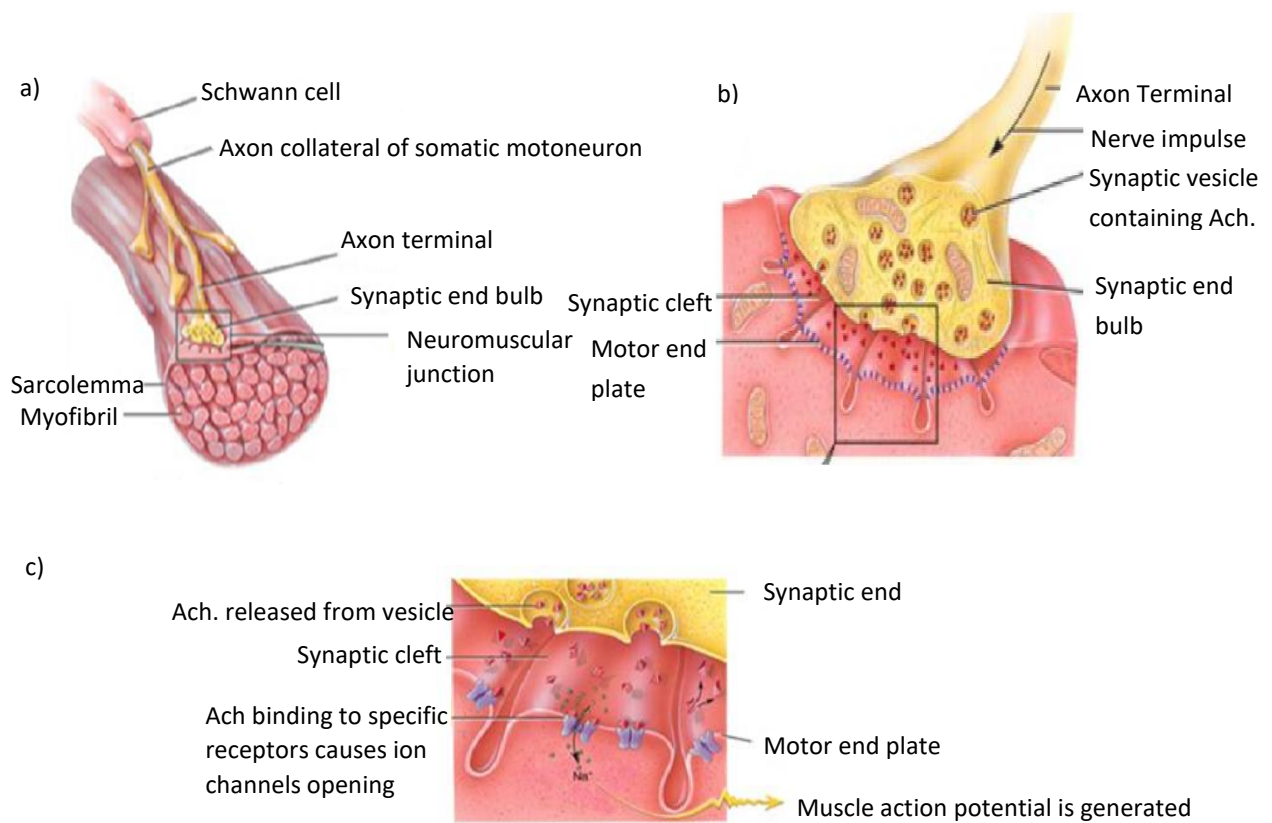


Figure 2.1.2: a) general architecture of a muscle fiber; b) close-up on the neuromuscular junction; c) acetylcholine binding mechanism

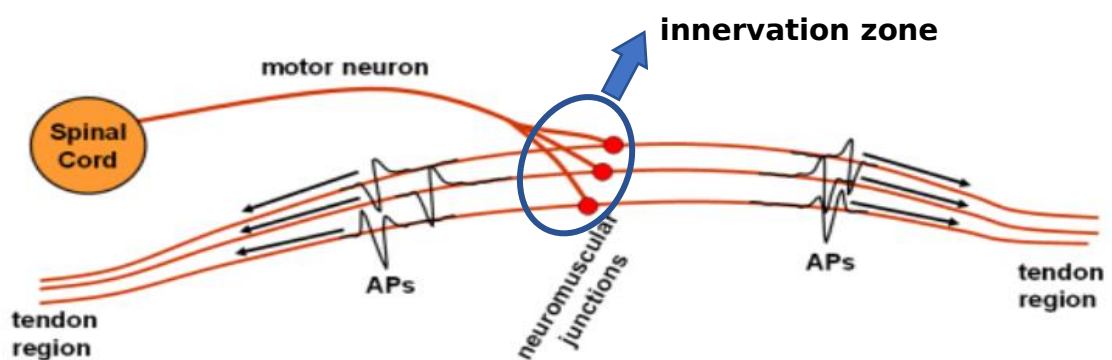


Figure 2.1.3: simple representation of a generic innervation zone

Myoelectric potentials can be modelled as a triplet of charges, two negative and one positive whose total charge intensity is actually null: once the first negative charge arrives on the tendon, the positive one balances its charge and makes it disappear. Since the positive one is the most intense, there is still a remaining positive charge to be extinguished: that's when the second negative charge comes in and completes the compensation of the three charges. The whole process is detected under the active electrodes as a high-intensity common mode effect called 'end-of-fiber effect' (fig. 2.1.4).

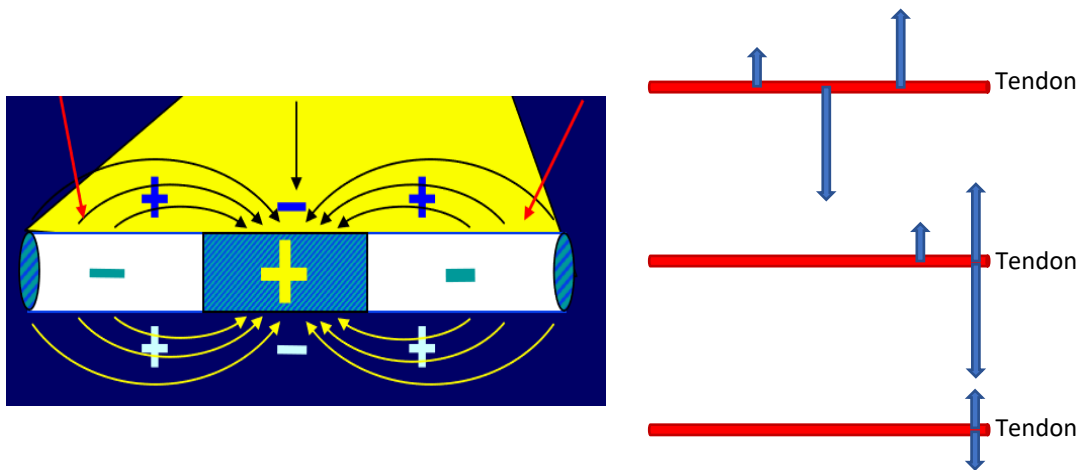


Figure 2.1.4: end-of-fiber effect: representation of a myoelectric potential as a triplet of charges; as it can be seen on the right, potentials from the triplet compensate each other once they reach the tendon.

2.2 Introduction to surface EMG and comparison with iEMG

Medical staff and researchers have carried out clinical analysis and studies relying on intramuscular EMG for decades. This form of acquisition requires the introduction of a wire or needle electrode into the patient's muscle: on one hand it provides a very spatially localized acquisition, on the other it can also damage muscle fibers involved in the acquisition and therefore cause pain to the patient. This first issue related to intramuscular EMG has been solved thanks to V-shaped and curved wire electrodes that can be wrapped around the muscle fiber without damaging it and still acquire the biopotentials on that fiber.

However, a major drawback is the invasive nature of this technique, which is not always tolerated by patients nor it can be easily applied in many dynamic conditions (such as sport movements).

The lack of a more patient-friendly practice to acquire and analyse EMG signals has led to the development of a new kind of technique in more recent years: surface EMG (sEMG in short).

In this technique, electrodes are positioned just on the patient's skin and they are typically Ag or Ag-Cl bipolar electrodes: this means that they define a certain area under the patient's skin from which EMG is acquired.

This area is called acquisition volume: it is usually modelled as a hemisphere whose radius is approximately equal to the interelectrode distance. Therefore, sEMG is a combination of all the potentials coming from all the muscle fibers contained in the acquisition volume. This is one of the main advantages of this technique, as well as its non-invasive nature. However, sEMG is also known as a signal of 'interference', as described in the picture below (figure 2.2.1).

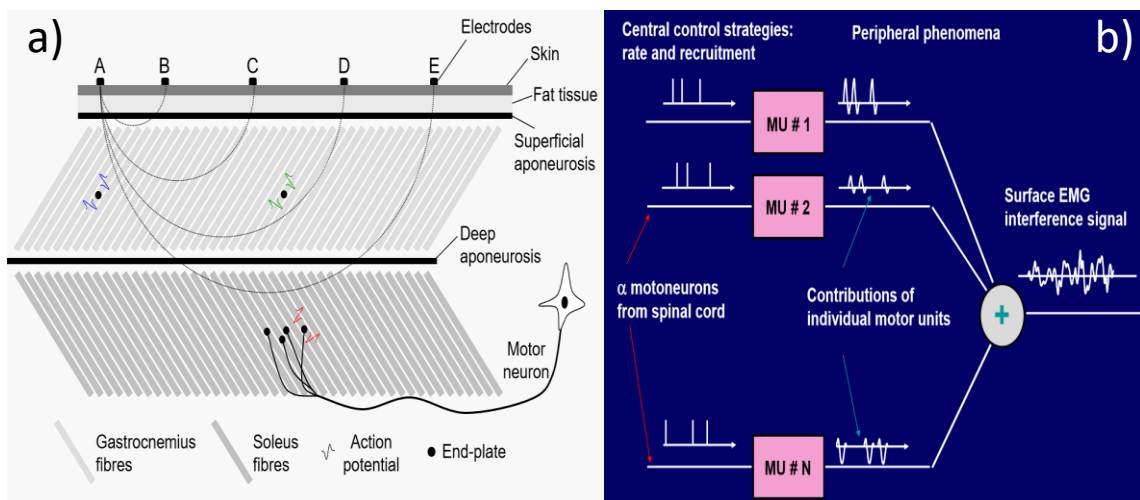


Figure 2.2.1: a) concept of detection volume: a higher interelectrode distance guarantees access to a larger number of motor units, but it might lead to crosstalk as well; b) sEMG is an interference signal made up of all potentials coming from muscle fibers which have been detected within the detection volume.

Every motoneuron sends electrical impulses to each muscle fiber under its control and each so generated potential is called motor unit action potential (MUAP). The sum of all MUAPs is sEMG, so interpreting such a complex signal is quite challenging, since each MUAP 'interferes' with all the others. Moreover, since the acquisition volume grows larger with a higher

interelectrode distance, the higher the distance between the electrodes is, the more fibers will be contained in the acquisition volume and the more interference there will be. Interelectrode distance is then a key parameter in sEMG acquisition which must be adjusted accordingly to the goals of the carried out clinical analysis. A too much high interelectrode distance may cause an acquisition of a combined myoelectric activity coming from both muscle fibers of interest and other fibers of nearby muscles: this is called 'crosstalk' and it must be avoided to perform a correct sEMG acquisition.

Another critical aspect to be checked in every sEMG acquisition is skin preparation. The subject's skin can be seen as a boundary line dividing an insulating semispace (air) from a conductive and anisotropic semispace (muscles, subcutaneous layers, etc.); it's mainly composed of electrolyte solutions in which current is carried by ions, just as it happens with muscle activity, while metal electrodes are crossed by electrons currents. This is why this environment is intrinsically noisy. The patient's portion of skin covering the muscles of interest must be then cleaned and scrubbed and hair must be removed to guarantee a high-quality skin-electrode interface. If skin preparation is not executed adequately, signals can be acquired with a low signal-noise ratio and potentials propagation might not be clear.

In any case, however, in any sEMG acquisition electrical sources of muscle activity are quite far from their detection point, which is on the skin; that's why underlying tissues have a low-pass filter effect on detected potentials which cannot be avoided. This effect makes potentials appear delayed and more dilated in terms of shape if compared with acquired intramuscular MUAPs (fig. 2.2.2).

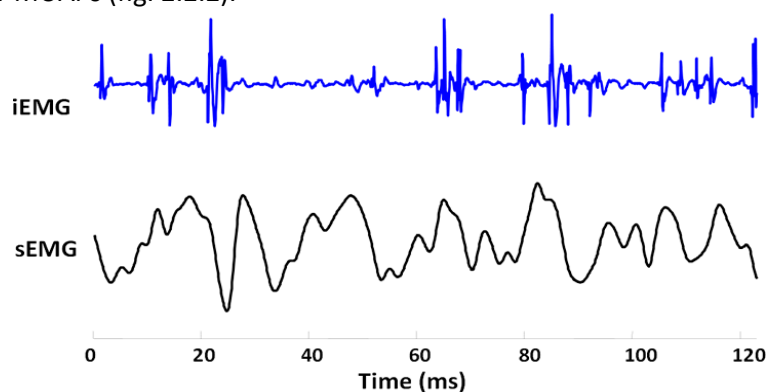


Figure 2.2.2: comparison between MUAPs acquired with needle invasive electrodes (above) and bipolar surface electrodes (below): potentials acquired at skin level are visibly smoother and slower than those detected invasively.

To sum up, intramuscular EMG is definitely more spatial-specific than sEMG, but it's not so easily performable in all dynamic conditions due to subject's pain and potential danger for the muscle fibers. On the other hand, sEMG needs a higher grade of experience to be interpreted correctly and it also requires a more complex and longer preparation of both experimental set-up and patient, but it's completely pain-free.

2.3 sEMG detection configurations and spatial filters

sEMG is usually acquired by means of multiple electrodes configurations, here listed and represented (fig. 2.3.1) below:

- Monopolar (MP): signals are detected with amplifier's reversing terminal connected to reference and non-reversing terminal to the detecting electrode;
- Single differential (SD): amplifier's reversing terminal is now connected to a second active electrode and the amplifier's output will be the algebraic sum of the two detected signals. In multichannel bipolar acquisitions, where not only a couple, but many couples of electrodes are used, N-1 single differential signals will be obtained from N active electrodes.
- Double differential (DD): a second group of differential amplifiers is added to the first one found in SD acquisitions. This results in double differential signals which will be the algebraic sum of the previous SD signals.

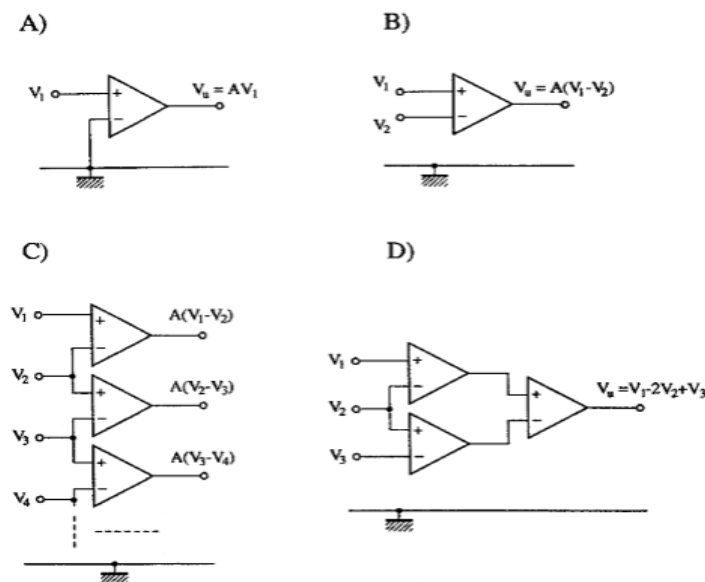


Figure 2.3.1: possible configurations for sEMG detection: a) monopolar (MP); b) single-differential (SD); c) cascade of single-differentials; d) double-differential (DD).

Each of these configurations has specific advantages which make them appropriate to analyse particular features of sEMG.

Information about firing patterns and instants can be extracted from monopolar signals. Monopolar detections contain major common mode components, among which 'end-of-fiber effect' (EoF) is a most important one. As brought up before (see Chapter 2.1, pag.8), myoelectric potentials die out when they reach the tendon. The 'EoF effect' might be interesting to analyse since it can reveal the true position of the muscle tendon, but it might also influence signal quality negatively because its high amplitude might cover EMG potentials. Single differential detection solves this problem out by filtering most of the common mode away and making the propagation of potentials more evident. However, SD signals usually fail to give a clear representation of firing patterns of motoneurons and firing instants.

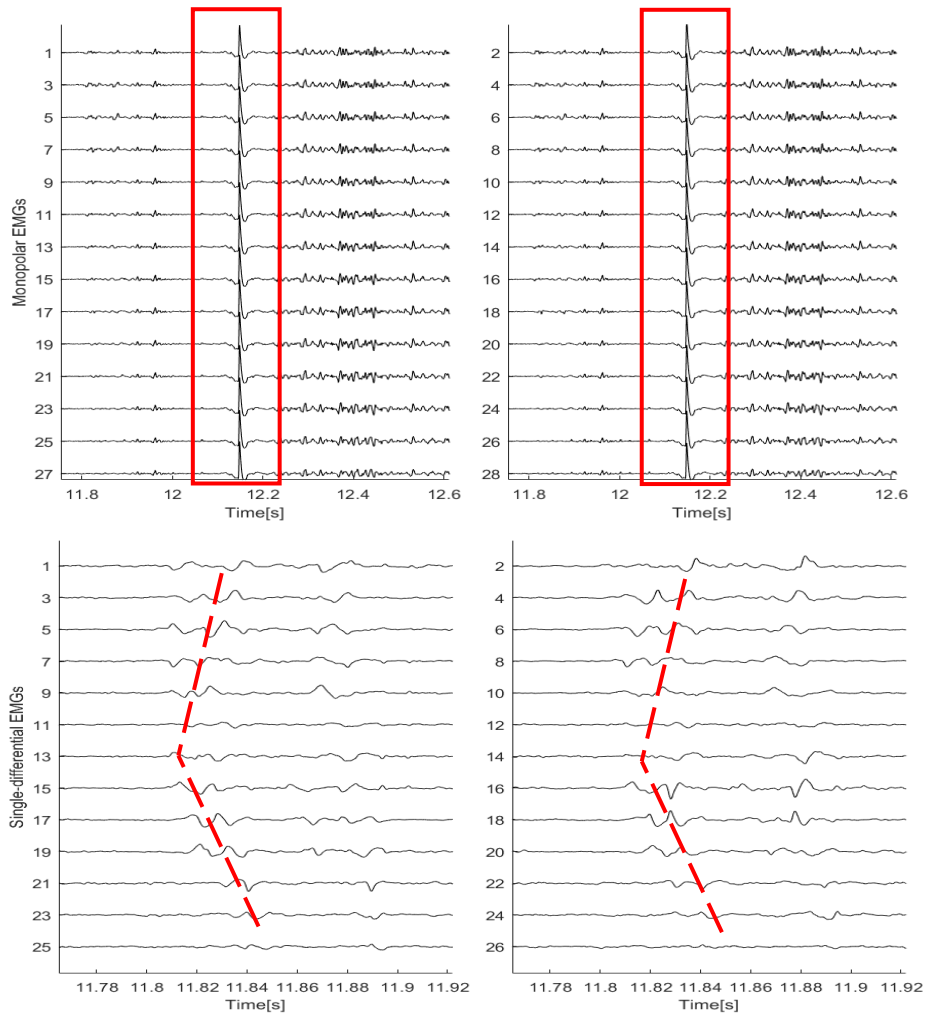


Figure 2.3.2: visual differences between MP and SD signals (signals have been recorded with a multichannel EMG detection system, with a sampling frequency of 2048 Hz and reorganized)

and post-processed in Matlab®, version 2017a); EMGs come from a male subject's right rectus femoris during gait. Channel 1 is in correspondence of the proximal end of the muscle, while channel 28 (or 26 in single differentials) shows activity from the farthest-possible distal portion. It must be noticed that in the first plot, monopolar EMGs clearly show 'end-of-fiber' effects as simultaneous potentials on every channel, while in the second plot single-differentials allow to distinguish clearly propagating potential.

Spatial filters are also an important part of sEMG processing and analysis, since they allow to transform a monopolar signal into a single differential one, cut the power line frequency interference off, reduce common mode components which affect signal quality and other disturbing factors. Spatial filters are the most modern technique of sEMG acquisition and processing: they are a combination of sEMG signals from different channels which are processed with a series of weights functions in order to obtain a linear combination explicative of sEMG trends. Every non-monopolar configuration is actually a specific spatial filter itself because it behaves differently according to the detected biopotentials under the subject' skin.

A single couple of bipolar electrodes can provide a good quality signal, but its related information might be insufficient to represent the entire muscle activity effectively. For this reason, high-density EMG is the upcoming sector in bioelectronics nowadays, since it allows to combine a set of electrodes and organise them in a matrix or array. This means being able to detect sEMG from multiple couples of electrodes simultaneously and having a wider spatial map of EMG distribution in a muscle.

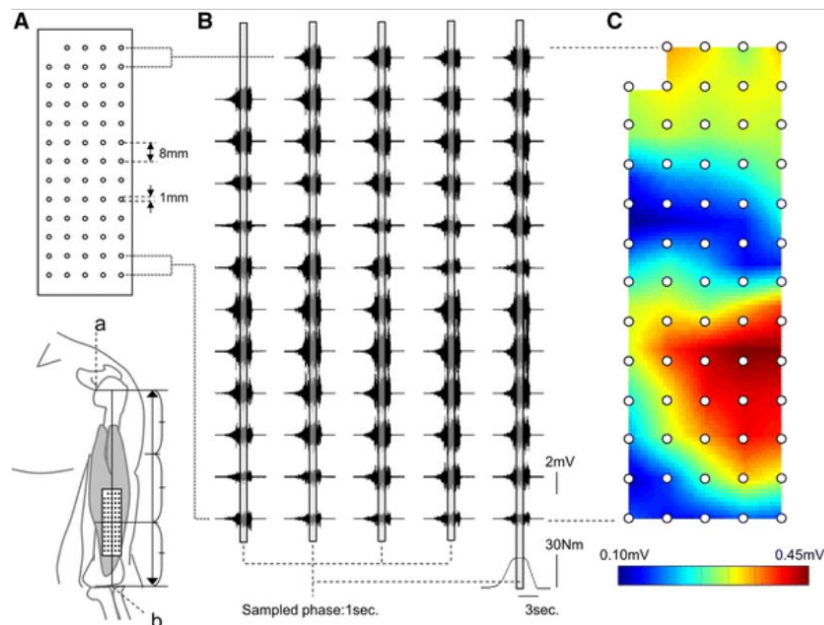


Figure 2.3.3: EMG spatial map acquired from a bicep muscle thanks to high-density EMG detection^[4].

3. Muscle synergies extraction

3.1 Concept of muscle synergies

Many investigators and researchers since Bernstein (1967) have acknowledged that when the Central Neural System (CNS) generates a voluntary movement, a significant number of different motor units and therefore muscles are activated simultaneously; this discovery has led to the hypothesis that the CNS manage both simple and complex movements with a little set of muscle modules, also renamed muscle synergies ^[1]. In other words, the CNS activate specific groups of muscles together to perform a certain task and each common task and exercise (gait, grasping and many others) have their own muscle synergy of reference and activation patterns of their respective muscles. Convincing evidence have shown that in several vertebral animal species ^{[5] [6] [7]} as well as in humans ^{[8] [9]} this simplifying control strategy is key to overcome redundancy of the skeletal system, activating the right muscle fibers for a specific action, otherwise the high number of muscle fibers which can be involved in certain tasks might lead to inaccuracies during muscle fibers recruitment. It has also been confirmed that muscle synergies are 'learned' throughout early childhood by toddlers and pre-schoolers and then shaped up and improved gradually until adulthood ^[10], majorly by means of intuition and visualization of certain movements. Therefore, it is safe to say that muscle synergies have a neural origin ^[11] and they can also be modified by CNS in critical situations (for example, a neural disorder or pathology ^[12]) in order to allow the completion of the required task.

3.2 Theory of muscle synergies: time-dependent synergies and synchronous synergies

Muscle synergies can be modelled as both temporal (or synchronous) synergies and time-dependent synergies ^{[7][13]*}.

The first model describes synergies as task-independent predefined muscles patterns, which are recruited selectively by different muscles according to the situation. Mathematically, a

* Since many works have taken advantage of this distinction between the two synergies models, please notice that these quotations express a preference only in terms of word selection and simplicity, NOT concepts, equally presented in all consulted and non-consulted works.

control input or temporal synergy $u(t)$ is conceived as a linear combination of $\{a(t)\}$ coefficients, which are task-independent muscle modules also known as activation coefficients, and $w(t)$, which are task-dependent control input vectors or commonly referred to as synergy weights (fig. 3.2.1).

$$u(t) = \sum_{j=1}^k a_j(t)w_j \quad (1)$$

In other terms, each vector w_j specifies a balance between the input variables (e.g., balance between muscle activations), and its coefficient $a_j(t)$ determines its temporal evolution.

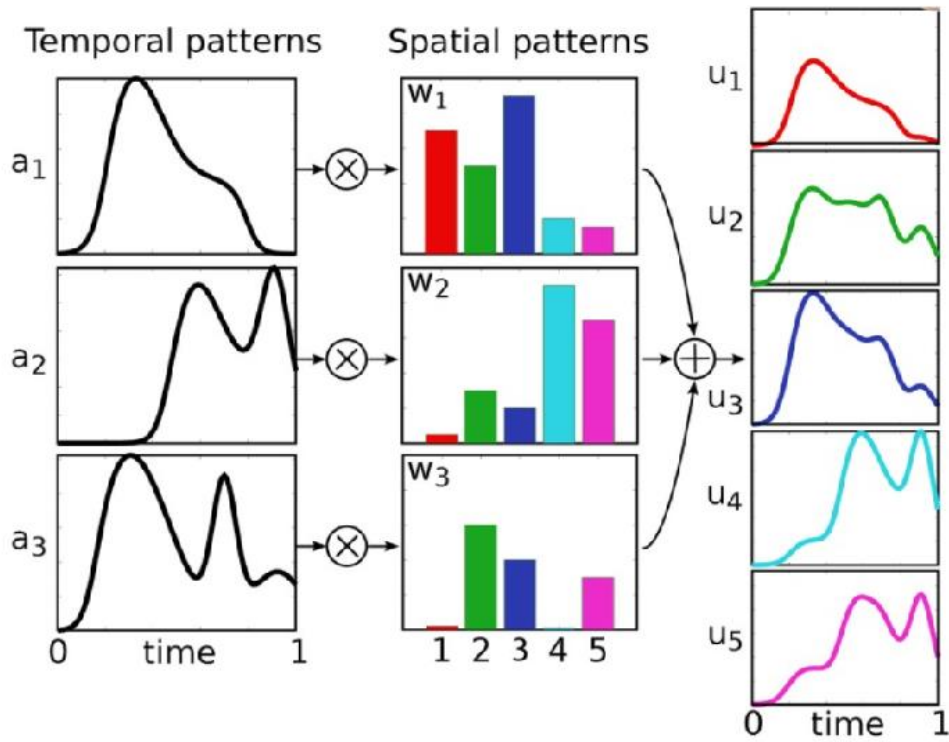


Figure 3.2.1: visual example of temporal muscle synergies extraction: temporal patterns (or activation coefficients) are linearly combined with spatial patterns (or weights); temporal patterns show activation levels of all muscles combined during the entire duration of a task (here normalized between 0 and 1), while spatial patterns are in the same number of analysed muscles (in this case, they are 5) and they indicate how much a muscle is active for that specific temporal pattern. As previously indicated in formula (1), u_j is then the sum of all a_j multiplied by its respective w_j .

On the other hand, the second model is about time-dependent or time-varying synergies: here, each synergy weight w_j can be scaled in amplitude and shifted in time thanks to coefficients a_j and τ_j , which must be specific for every different task (fig. 3.2.2).

$$u(t) = \sum_{j=1}^k a_j w_j(t - \tau_j) \quad (2)$$

These synergies are real spatiotemporal activation patterns which don't need any spatial or temporal separation, hence muscles involved in the same time-varying synergy do not necessarily change.

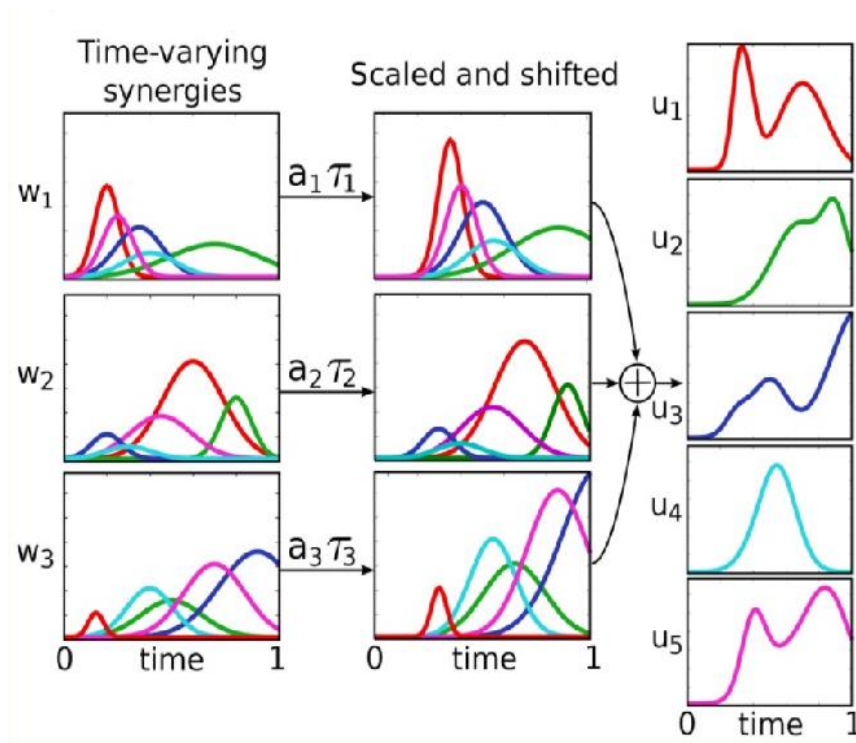


Figure 3.2.2: visual example of time-varying muscle synergies extraction: here all extracted muscles modules w_i are not just activation coefficients anymore, but they are already complete synergies containing both spatial and temporal information; however, additional scaling and shifting are required to map the entire muscular activity of interest.

In this thesis, synergies will be modelled as temporal according to the first model's parameters and any simulation presented from now on will be based on this model only. This

decision has been taken since the chosen extraction algorithm for the purposes of this thesis works well with synchronous synergies ^{[7][9]}.

3.3 Muscle synergies extraction algorithm: NNMF

In literature, many algorithms for extracting muscle synergies have been tested and confronted ^[13], in particular second-order blind identification (SOBI), principal component analysis (PCA), non-negative matrix factorization (NNMF) and independent component analysis (ICA). A. Ebied et al. have proven in their work that while SOBI is the best solution if the number of channels at disposal is limited, high number of channels/number of synergies ratio is a vital parameter to obtain a reliable extraction and with a satisfying ratio NNMF has been chosen as the most effective algorithm. This is the reason why all simulations carried out in this thesis are based on NNMF.

Basically, this algorithm is useful to reduce a dataset's dimensions by dividing it into subsets of information and extracting key hidden features of this dataset. Recombining all the extracted subsets, the original dataset is again obtained. From a mathematical point of view, synergies extraction running NNMF as the chosen algorithm can be represented as follows:

as inputs, this algorithm takes a matrix containing sEMG signals, whose dimensions are $m \times t$, where m is the number of analyzed muscles and t is the duration of a single sEMG signal, and k , number of extracted synergies (to be specified beforehand). Two aspects must be pointed out though: here it is assumed that there is only one detection channel for each muscle and, since Matlab® 2017a is the chosen software to support the algorithm and digital signals are never continuous, but always discrete, t is to be considered as a duration expressed in samples and not seconds. The NNMF algorithm will extract k synchronous muscle synergies from the original matrix, separating it in two sub-matrixes as follows (also see fig. 3.3.1):

- spatial patterns or synergies' weights matrix, also commonly referred to as matrix W , whose dimensions are $m \times k$, with m number of involved muscles and k number of extracted synergies.

- temporal patterns or activation coefficients' matrix, also commonly referred to as matrix H , whose dimensions are $k \times t$, with k number of extracted synergies and t number of samples.

The vector product $W \times H$ defines a new matrix $sEMG'$, which is equal to the original $sEMG$ matrix except for an error, due mainly to noise. Therefore,

$$sEMG' = \sum_{j=1}^k w_j h_j(t) \quad (3.1)$$

$$sEMG = \sum_{j=1}^k w_j h_j(t) + e \quad (3.2)$$

$$sEMG(t) \approx W \times H(t) \quad (3.3)$$

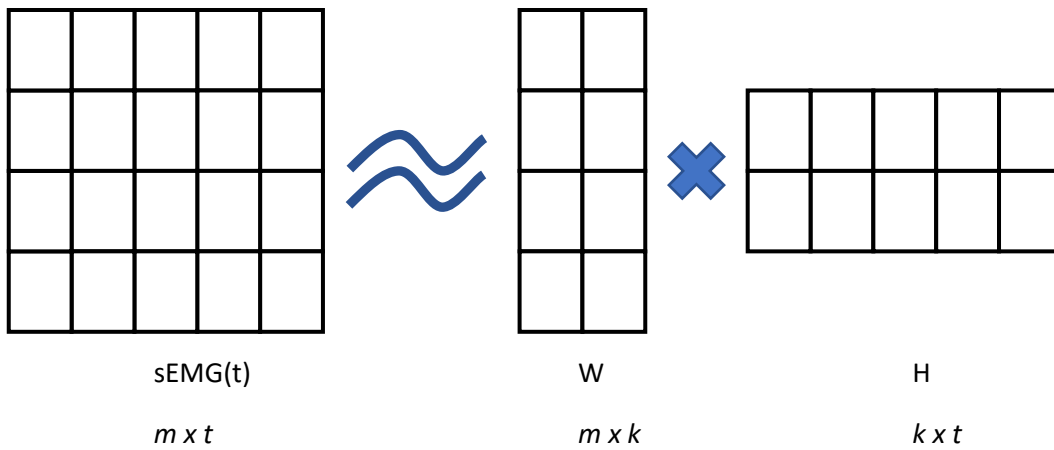


Figure 3.3.1: quick schematics of the factorization of the sEMG matrix, which is divided into W (synergies' weights matrix) and H (activation coefficients matrix).

NNMF algorithm is iterative and, as mentioned before, the number of extracted synergies must be defined before the algorithm is initialized. However, this is quite a drawback for this work's purposes, since adapting the number of extracted synergies according to different conditions, tasks and subjects is vital for a complete analysis.

A parameter which helps to choose the right number of synergies is then required and its update must occur at each NNMF run in order to verify if the chosen number is satisfying enough to represent the original sEMG matrix with a small error. If it's not, then the number of synergies must be increased for the following repetition of the algorithm. This parameter is *VAF* (Variance Accounted For), which describes how small the factorization error is and then how much the reconstructed signal, obtained as a linear combination of the synergies extracted by the algorithm, is different from the original one. VAF is formulated as follows,

$$VAF = 1 - \frac{\sum_{j=1}^k (M_j - M_j^R)^2}{\sum_{j=1}^k (M_j)^2} \quad (4)$$

where M_j indicates original sEMG signal associated with the j^{th} muscle and M_j^R is the reconstructed sEMG signal, calculated as the vector product of w_j and h_j . Since $\frac{\sum_{j=1}^k (M_j - M_j^R)^2}{\sum_{j=1}^k (M_j)^2}$ could never be higher than 1, VAF is a scalar which assumes values between 0 and 1: the lower VAF is, the worse the original sEMG signals are reconstructed. Here there is an example which shows how VAF values can be associated with the number of extracted muscle synergies (fig. 3.3.2):

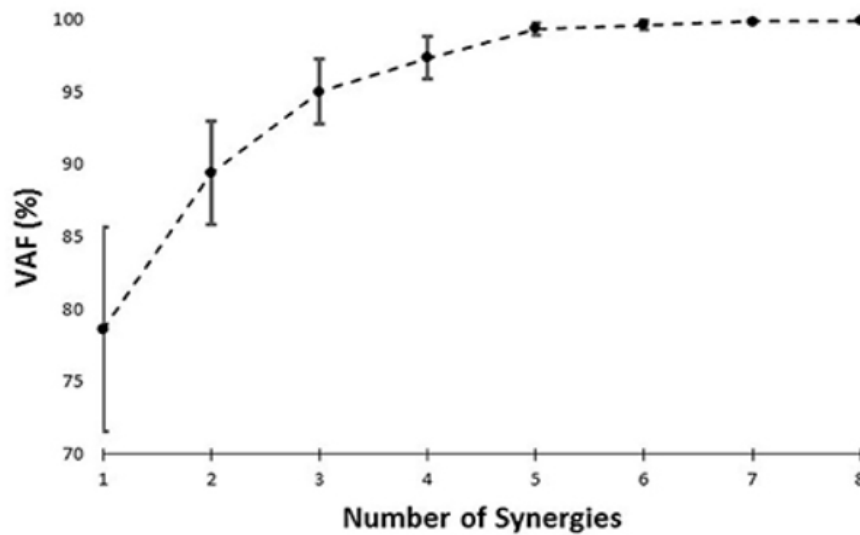


Figure 3.3.2: VAF values trend vs. number of extracted synergies: higher numbers of synergies lead to higher VAF values

Logically, higher numbers of synergies result in higher VAF values, since more synergies allow to find deeper details in activation patterns and rebuild sEMG signals better. However, since a VAF value equal to 1 is not necessary and many details in activation patterns can be seen as negligible, in literature a VAF which is equal to 0.9 [12][15][18] or 0.95 [16][17] is commonly an acceptable threshold and the ultimate chosen number of synergies will be the one in correspondence of these VAF values (this is called the ‘threshold criterion’ to select the number of extracted synergies and it is the most adopted and simple method).

3.4 Muscle synergies extraction during gait and bike: previous studies shown in literature

Many studies about muscle synergies extraction during gait and cycling have investigated synergies' numerosity and features during these two common tasks.

Typically, four to six synergies are found (Barroso et al. ^[20] (see Fig. 3.4.1), Clark et al. ^[25], Cappellini et al. ^[29]) for gait analysis and even though there are some methodological differences in EMG pre-processing and VAF values adaptation, a set of four common muscle synergies stands out:

- during early stance, a first synergy controls hip abduction and flexion as well as ankle dorsiflexion through Gluteus Medius and Tibialis Anterior; Vastus lateralis and medialis are also partially involved at increased gait speed;
- a second synergy reveals two peaks of activation during midstance and early swing due to Rectus Femoris' role as a knee extensor and hip flexor; a minor contribution comes also from Tibialis Anterior and Vastus Medialis;
- in a third commonly found synergy, Gastrocnemius Medialis and Soleus act as ankle plantarflexors during late stance, specifically during push-off;
- a final fourth synergy shows Biceps Femoris and Semitendinosus' activities: they are mainly involved during late swing through initial stance.

Synergies 5 and 6 usually represent further details of the second and third synergies respectively, showing specific involvement of Tibialis Anterior, Soleus and Gluteus Medius throughout the entire gait cycle duration. These activation modules are commonly added to the previous four to enhance EMG reconstruction quality, which would be less effective without them. However, they do not provide with any further information about neural control strategies.

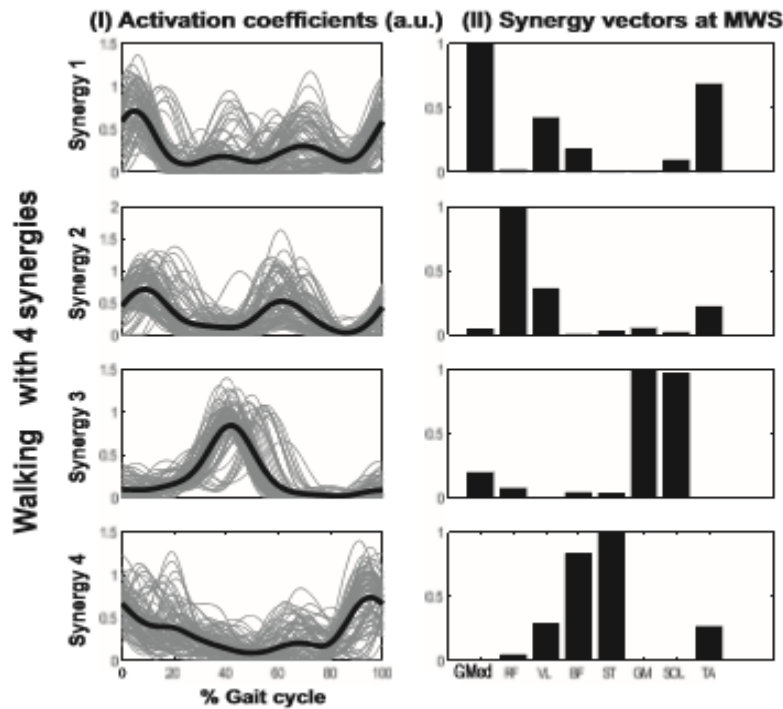


Figure 3.4.1: Barroso et al. [20]' study about muscle synergies in gait; synergy 1 and 2 principally describes muscle activations during the stance phase, while synergy 3 and 4 are prevalently relative to the swing phase. In this work, synergies have been extracted concatenating EMG signals from consecutive gait cycles and in this picture average-cycle activation coefficients are plotted along with synergy vectors. Abbreviations are associated with analysed muscles and these are GMed (Gluteus Medius), RF (Rectus Femoris), VL (Vastus Lateralis), BF (Biceps Femoris), ST (Semitendinosus), GM (Gastrocnemius Medialis), SOL (Soleus) and TA (Tibialis Anterior). Gait was performed on a treadmill in this study.

Cycling has also been investigated in several studies (Barroso et al. [20] (see Fig. 3.4.2), Hug et al. [30], Barroso et al. [31]) and it can be stated that three synergies are predominant since they allow to reconstruct successfully a significant part of the original EMG content. Considering the bottom end centre as the beginning foot position for each cycle, the three synergies can be described as follows:

- the first synergy represents mainly Tibialis Anterior and, to a lower extent, Rectus Femoris, Gluteus Medius and Soleus and it basically shows muscles activation during the upstroke phase;

- the second synergy is made up of Rectus Femoris, Vastus Medialis and Soleus' activities and it's typically related to the end of upstroke and the initial downstroke phase;
- Biceps Femoris and Gastrocnemius Medialis principally belong to the third synergy, which is associated with the downstroke phase.

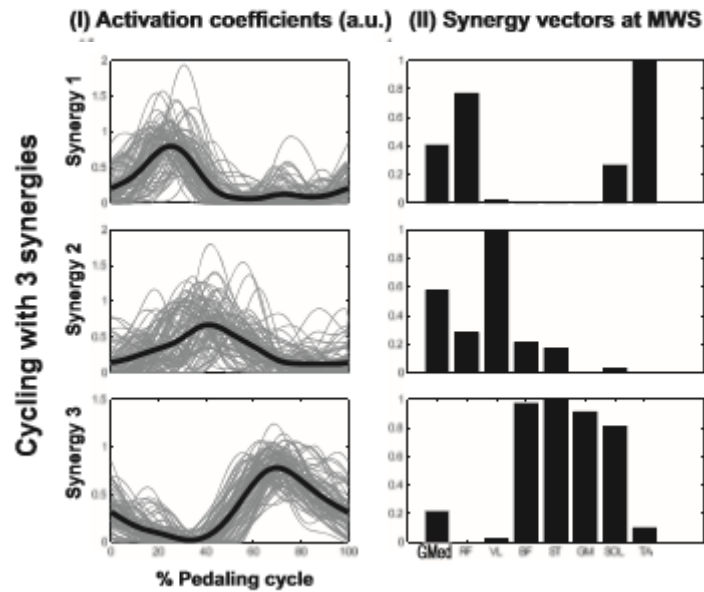


Figure 3.4.2: Barroso et al. ^[20]'s study about muscle synergies in cycling; synergy 1 is involved during the upstroke phase for the most part, synergy 2 refers to the end of upstroke and beginning of downstroke, synergy 3 shows muscle activation patterns during most of downstroke. In this work, synergies have been extracted concatenating EMG signals from consecutive cycles and in this picture average-cycle activation coefficients are plotted along with synergy vectors. Abbreviations are associated with analysed muscles and these are GMed (Gluteus Medius), RF (Rectus Femoris), VL (Vastus Lateralis), BF (Biceps Femoris), ST (Semitendinosus), GM (Gastrocnemius Medialis), SOL (Soleus) and TA (Tibialis Anterior). Gait was performed on a treadmill in this study.

4. Materials and methods

4.1 Subjects

Experiments were carried out on 8 healthy male subjects (age: 29.1 ± 10.7 years, height: 177.3 ± 3.2 cm, body mass: 72.2 ± 7.8 kg). Before starting any trial, each subject was instructed properly about the protocol and was asked to sign an informed consent. Since measurements involve only one limb, every subject's dominant leg was always the one instrumented.

4.2 Experimental protocol

As a first trial, each subject was asked to walk over ground. Since walking must be at a comfortable pace, yet not excessively slow, every subject was asked to walk at self-selected speed across a 10-m long corridor, maintaining a certain degree of effort to still allow complete muscular engagement from all the districts of lower limb. This walk was repeated 5 times and each time the subject was asked to stop for three seconds, turn around, stop for other three seconds and then start walking again. Average self-selected gait speed among all subjects was 3.8 ± 0.4 km/h.

After walking, 1 minute of cycling was then performed on a stationary bike, at 40 rpm and with the same fixed resistance (100 W) for every subject. This resistance was chosen as a good compromise between level of effort and simplicity of the task.

4.3 Materials and skin preparation

Materials which were employed during trials are (also see fig. 4.3.1 and 4.3.2):

- *Meacs*[®] (high-density EMG detection system)
- *Due*[®] (bipolar EMG detection system)
- *DueBio*[®] (biomechanical probe)
- 32-electrode arrays and matrices
- Disposable bipolar electrodes
- Foam

- Reference electrodes and wires
- Conductive paste
- Abrasive paste
- Foot switches
- Electrogoniometer
- Treadmill (Reharunner 01™ by Chinesport™)
- Stationary bike (Cyclette BRX Easy™ by Chinesport™)
- *Bp*® (software for online signals visualisation)

Flexible Kapton® 16x2-electrode arrays were adopted, which allows to have 32 channels for each muscle at disposal.

A DUEBio® probe was employed to monitor biomechanical signals, which come respectively from two foot switches for gait (one on the first metatarsal head and the other on the heel) and from an electro-goniometer for bike (positioned across the knee joint).

Signals were visualised offline on *bp*®, a software for offline EMG signals visualization and post-processing adaptable to both high-density and bipolar EMG.

The EMG multichannel detection which we have worked with is called Meacs (Multichannel EMG Acquisition System), produced by LiSiN (*Laboratorio di Ingegneria del Sistema Muscolare*), Turin. It is a wearable system expressly thought to acquire sEMG and monitor myoelectric activity. The system has 32 detection channels, with 3 other channels to perform other measurements and it's able to communicate via Wi-Fi with a PC for both online and offline signal visualisation.

Subject' skin was specifically treated to ensure EMG maximum possible quality (see appendix C for a complete description of the process).

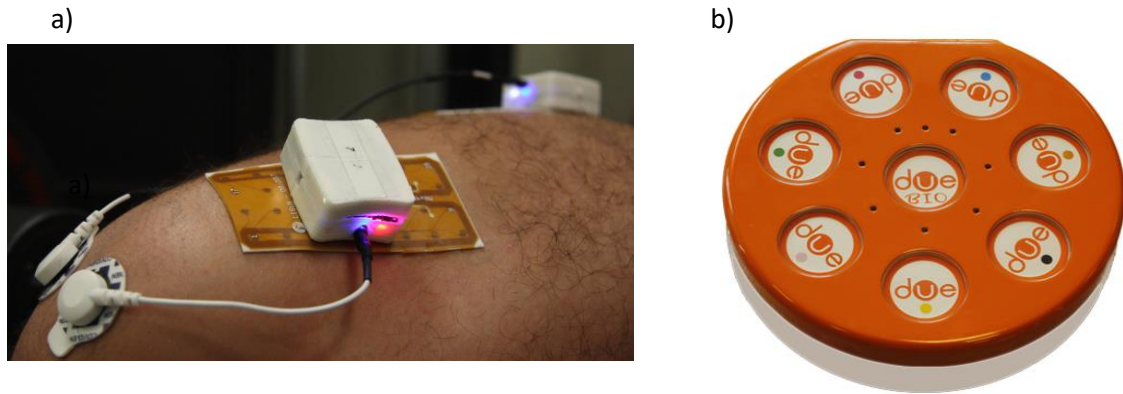


Figure 4.3.1: High-density EMG detection system (MEACS) applied on a subject (a), EMG bipolar and biomechanical probes (Due and DueBIO) (b)

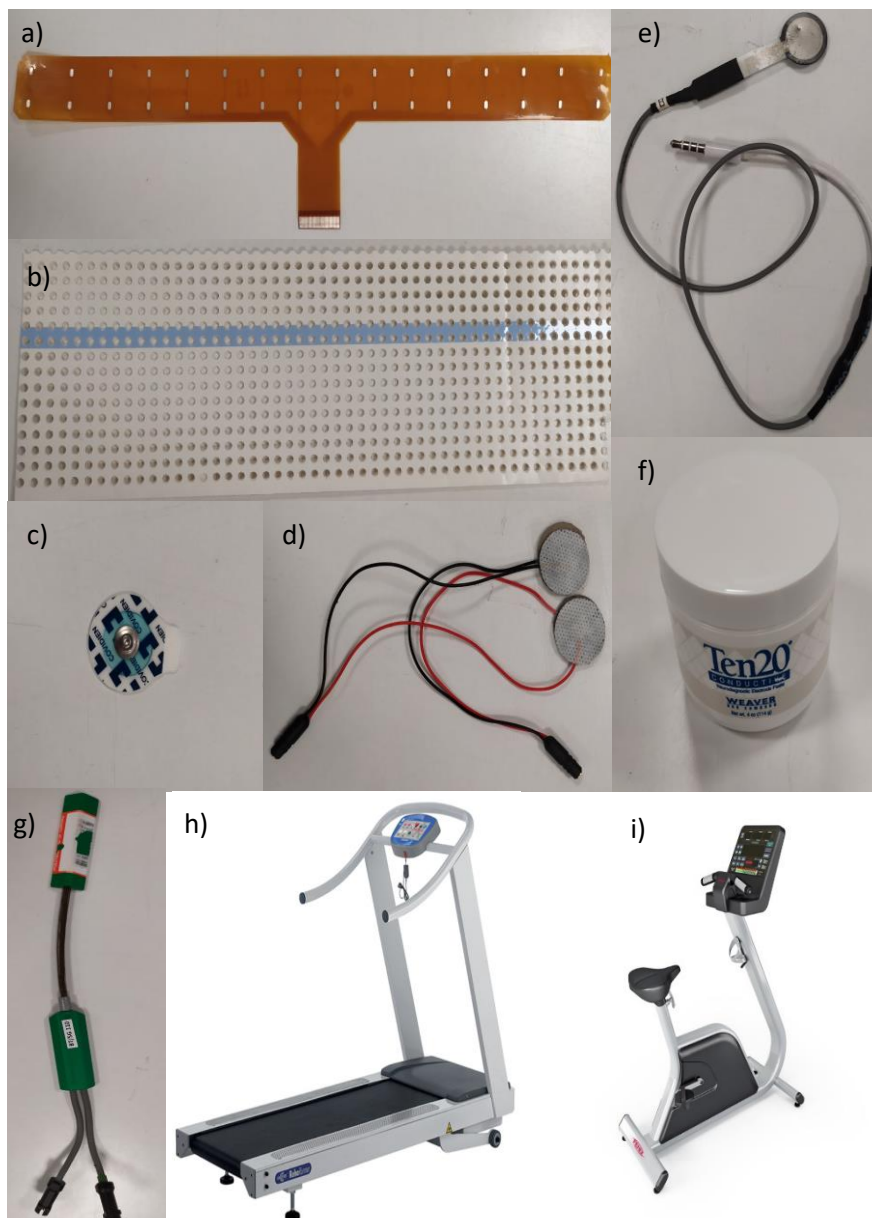


Figure 4.3.2: a) detection EMG 1.5cm IED 16x2 array; b) foam; c) reference electrode; d) bipolar detection EMG electrodes; e) force sensor used as foot switch; f) conductive paste; g) electro goniometer; h) treadmill; i) stationary bike

4.4 Selected muscles

Chosen muscles for this study are reported below with a specific reference to those works which present differences in their fibers' orientation and functional behaviour:

- Rectus Femoris is a long pennate muscle whose proximal region has been confirmed by K. Watanabe et al. ^{[1][31]} to be more activated during hip flexion, while its distal end is more involved during knee extension (fig. 4.4.1);

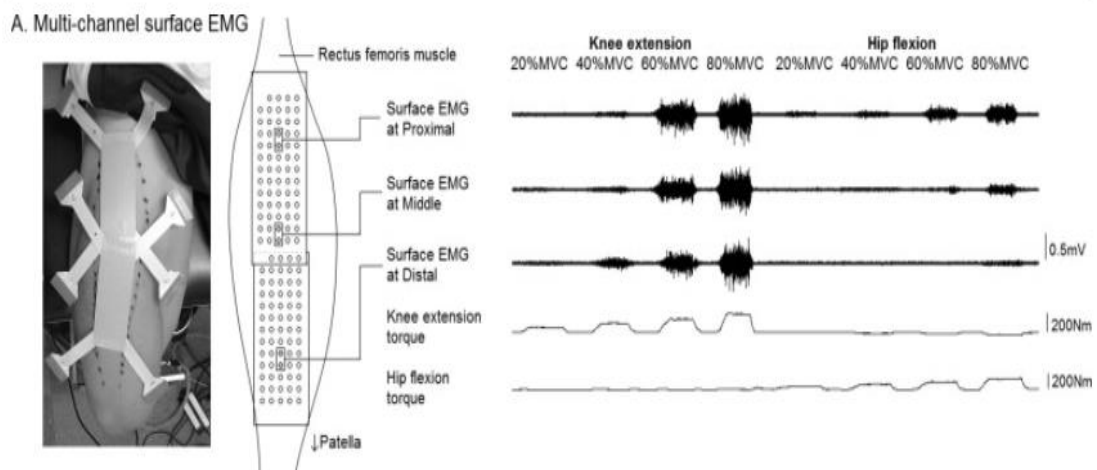


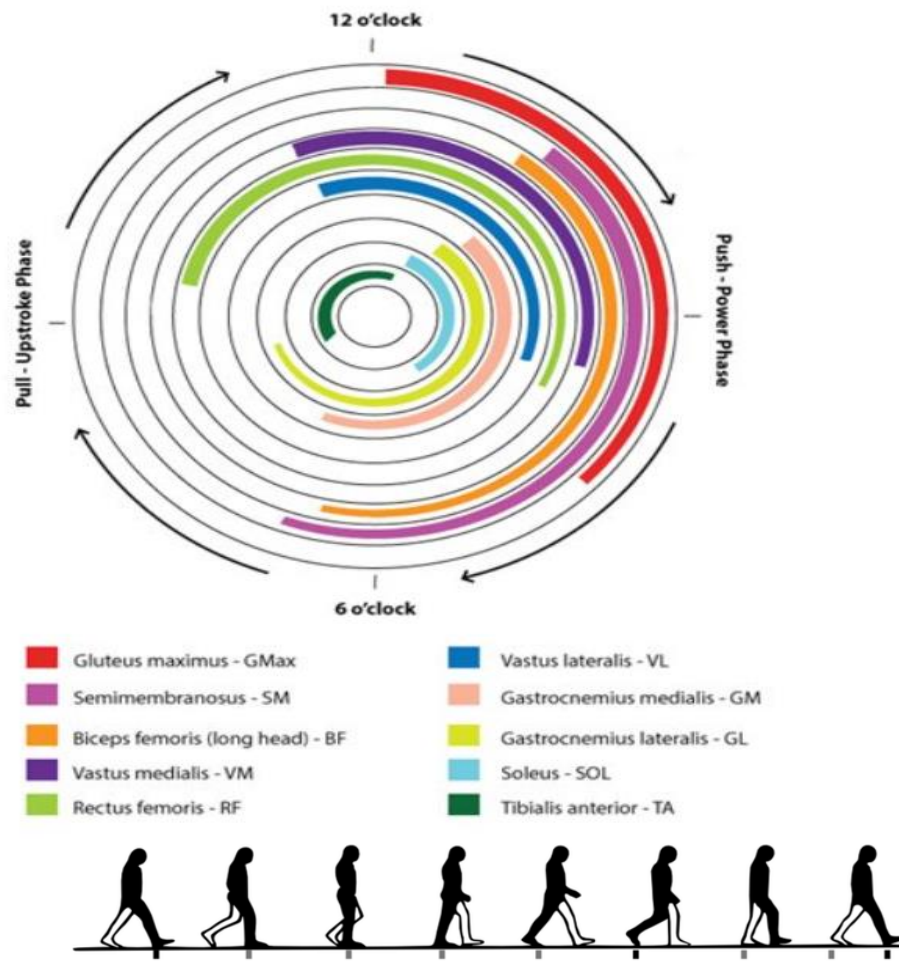
Figure 4.4.1 (picture from Watanabe et al. ^[31]): Watanabe et al. ^{[1][34]} studied how rectus femoris seems to behave differently according to the task phase of interest. Its proximal region seems to be more involved during hip flexion, while distal region is definitely more active during knee extension. Mapping this muscle with high-density EMG is then vital to spot its internal different behaviours.

- Vastus medialis was deeply studied by H.V. Cabral et al. ^[2] and they found out that discharge rates of motor units in the proximal portion of the muscle are much more cross-correlated to other neighbouring motor units rather than those in the distal portion. This result suggests that these two sectors of the vastus medialis could be modulated differently and their functional roles can also be considered as independent according to A. Gallina et al. ^[22].
- Soleus' anatomy was Staudemann et al. ^[23] 's main interest in a specific research which confirms that this muscle's medial and lateral portion are selectively operative

during foot eversion and inversion respectively and this can have some involvement even in free gait.

From now on, each other muscle has been chosen since it gives a significant contribution to both gait and cycling, even though it doesn't have such a marked distinction in its architecture or function:

- Gluteus Medius, majorly involved in gait as hip flexor and abductor at the beginning of the cycle (considering heel strike as the starting phase), during early stance, while in cycling it is important during early and late upstroke;
- Biceps Femoris, which is a knee flexor and hip extensor that is engaged during the terminal phase of swing; in cycling it is the principal actuator during downstroke;
- Tibialis Anterior is an important coactivator of rectus femoris as ankle dorsiflexor during early stance; it is greatly involved in cycling during the final upstroke phase;
- Gastrocnemius Medialis has a significant role in late stance as well as soleus, whereas in cycling it is activated between final upstroke and initial downstroke.



	Stance phase					Swing phase		
	Double support	Simple support			Double support			
		Initial	Middle	Terminal		Initial	Middle	Ter.
ILIACUS						■	■	
SARTORIUS						■	■	
GRACILIS	■					■	■	
RECTUS FEMORIS	■				■	■		■
ADDUCTOR LONGUS			■	■				
VASTI	■	■						
GLUTEUS MAXIMUS	■	■						■
GLUTEUS MEDIUS	■	■						■
BICEPS FEMORIS	■							■
TIBIALIS ANTERIOR	■	■			■	■	■	■
EXTENSOR DIGITRUM LONGUS	■				■	■	■	■
GASTROCNEMIUS		■	■	■				
SOLEUS		■	■	■				
FLEXOR HALLUCIS LONGUS			■	■				
TIBIALIS POSTERIOR		■	■	■				
PERONEUS LONGUS			■	■				

Figure 4.4.2: a compact graphical representation of muscles involved during cycling (above) and gait (below) during their respective cycle

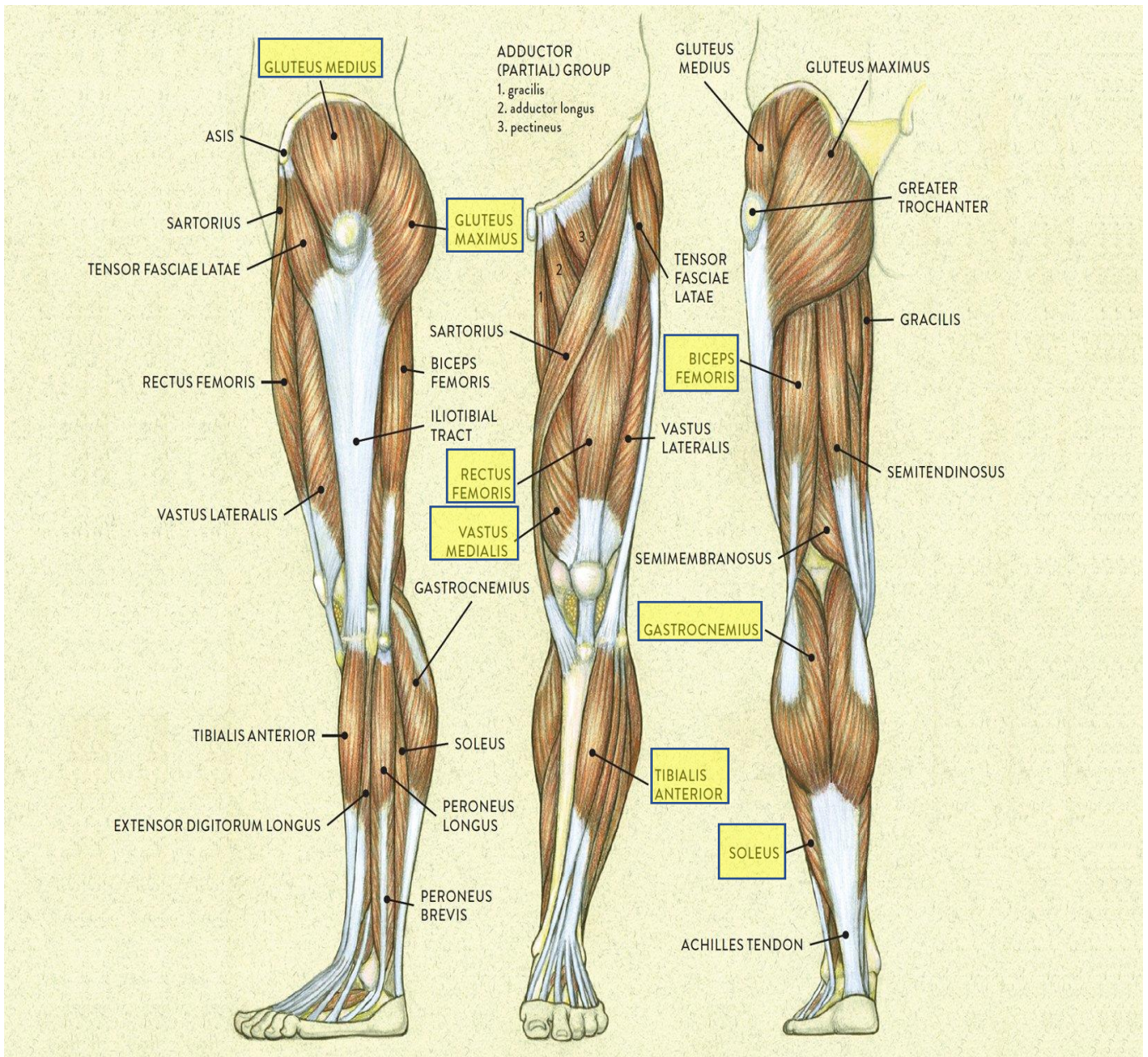


Figure 4.4.3: muscles involved in this study (highlighted in yellow)

4.5 Electrodes positioning

Each muscle requires precise electrodes positioning according to its fibers' orientation and organization (see Appendix A for a graphical presentation of how electrodes should be positioned on every muscle):

- Rectus Femoris: this muscle runs along almost the entire length of the femur, so since its proximal and distal regions are to be analysed separately, a long array to detect

EMG is the right solution. A 16x2 electrodes, 1.5 cm interelectrode distance array is then placed on the subject's thigh, starting from the distal end of the muscle (identified both observing it and by palpation). An ideal line to establish the correct array orientation is the one going from the iliac crest bone to the patella, as suggested by Watanabe et al. ^[1].

- Vastus medialis: a couple of bipolar electrodes is placed on its proximal portion, whose fibers define a slight angle with the longitudinal axis of the thigh; on the other hand, since fibers closer to the patella progressively increase their pennation angle, a new couple of electrodes is placed transversely with respect to the first one ^[2]. Best IED is 3-4 centimetres, as shown in Gallina et al. ^[23].
- Soleus: F.V. Dos Anjos et al. ^[3] show precise indications in their study for an effective electrode positioning for this muscle; at first, the distal end of the medial gastrocnemius is identified. Then, the upper electrode of the couple is positioned a few millimetres below this point, while the other electrode is placed at 45 degrees towards the inside of the lower portion of the muscle, 3 centimetres below the first electrode. Suggested IED is then 3 centimetres. The same indications are valid for both medial and lateral regions.
- Tibialis Anterior: a single bipolar electrodes couple is sufficient in this case and it must be positioned on the proximal end of the muscle, which starts a few centimetres below the patella. Proximally, TA's fibers undergo a sharp change in their inclination and they become parallel to the tibia. Another tip is to remain as close as possible to the tibia. A reasonable IED is 3 centimetres.
- Gastrocnemius Medialis: SENIAM ^[24] positioning was adopted; the electrodes couple must be positioned on the most prominent bulge of the muscle, right in the middle. IED is 2 centimetres and electrodes' orientation should follow the line which links the distal end of the muscle and the popliteal area.

- Gluteus Medius: SENIAM ^[24] positioning was adopted; electrodes should be placed in the middle of the imaginary line which connects the iliac crest bone and the trochanter. Suggested IED is 2 centimetres.
- Biceps Femoris: SENIAM ^[24] positioning was chosen, which means halfway between the ischial tuberosity and lateral epicondyle. Suggested IED is 2 centimetres.



Figure 4.5.2: complete experimental set-up applied on a subject

Before the beginning of any experimental acquisition of subjects following the complete protocol, a quick test on two different subjects was done to assess actual differences in rectus femoris and vastus medialis during different gait and cycling phases. At first, a 32x1-electrode, 0.5 cm IED array was chosen to detect EMG from rectus femoris, while two 8x4-electrode, 1 cm IED matrix were applied to vastus medialis' proximal and distal regions: these electrodes configurations allow to explore EMG spatial distribution effectively all along their extension. Notice that the first 8x4 matrix was placed along the proximal fibers, while the second matrix is positioned transversally on the distal portion of the muscle, so it will actually appear as a 4x8 matrix in fig. 4.5.4. What is likely to occur is a visible difference between activation instants of the proximal and distal portions of these muscles. Interestingly, it must be mentioned for both subjects that rectus femoris showed indeed different activation pattern and timing during separated task phases (fig. 4.5.3).

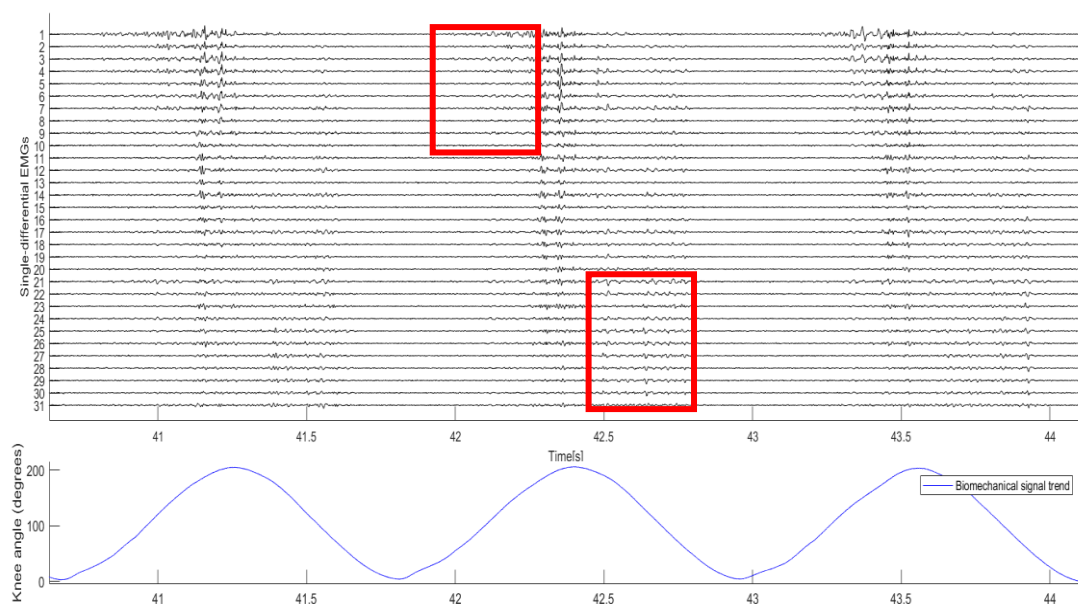


Figure 4.5.3: an example of single-differential EMGs from rectus femoris during cycling (please notice that the same difference occurs during gait): proximal regions (electrodes 1-10) seem to be more involved at the beginning of the task, while distal regions (electrodes 22-31) appear to be more active at the end.

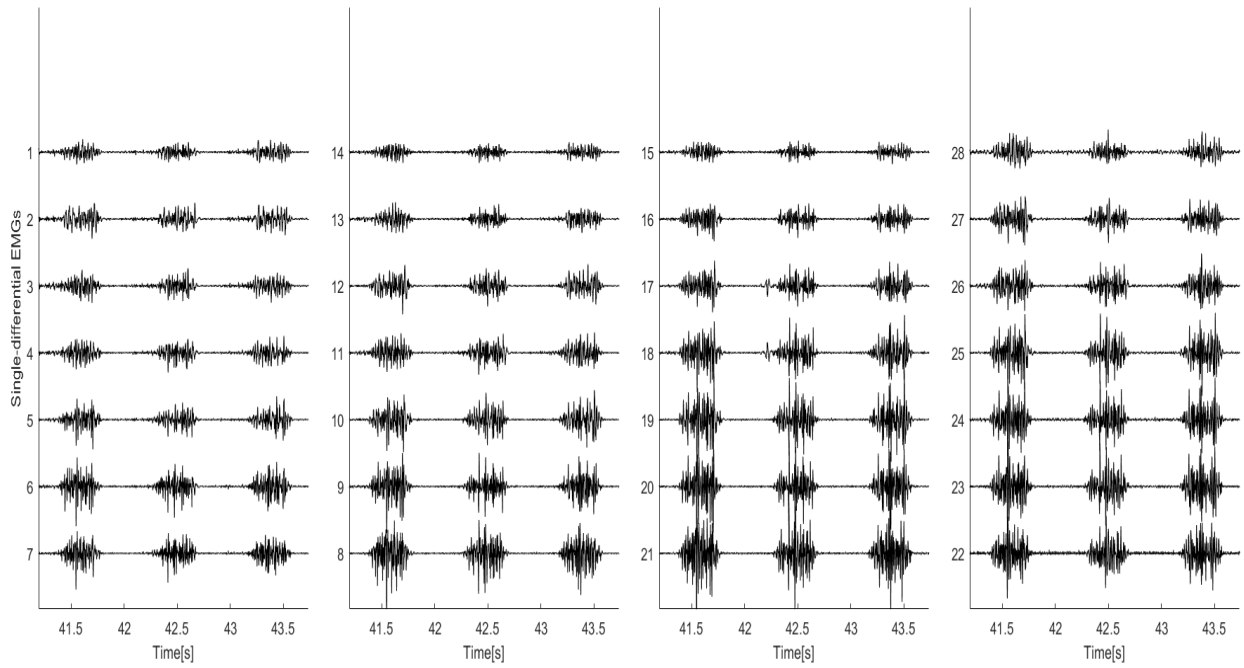
Since Rectus Femoris is a pennate muscle, exploring its transversal dimension was thought to be relevant as well. A 32x1-electrode, 0.5 cm IED array could be a drawback while mapping EMG activity along the entire muscle length, since it fits just about right to cover it completely and it provides valuable information only about those potentials which propagate

longitudinally. However, transversal single differentials would provide with information regarding more-region specific activity from both proximal and distal end of Rectus Femoris due to its conformation and fibers' orientation.

Therefore, a higher inter-electrodes distance and at least one more column of electrodes would be perfect. This is why a 16x2-electrode, 1.5 cm IED array was chosen.

On the other hand, concerning vastus medialis' proximal and distal ends, EMG potentials acquired from the same matrix were very similar, which could suggest that no actual difference in the same muscle region occurs (fig. 4.5.4). This test was also done to check if vastus medialis required a widespread EMG sampling by means of a matrix or if a bipolar electrodes couple was enough, which was our case.

a)



b)

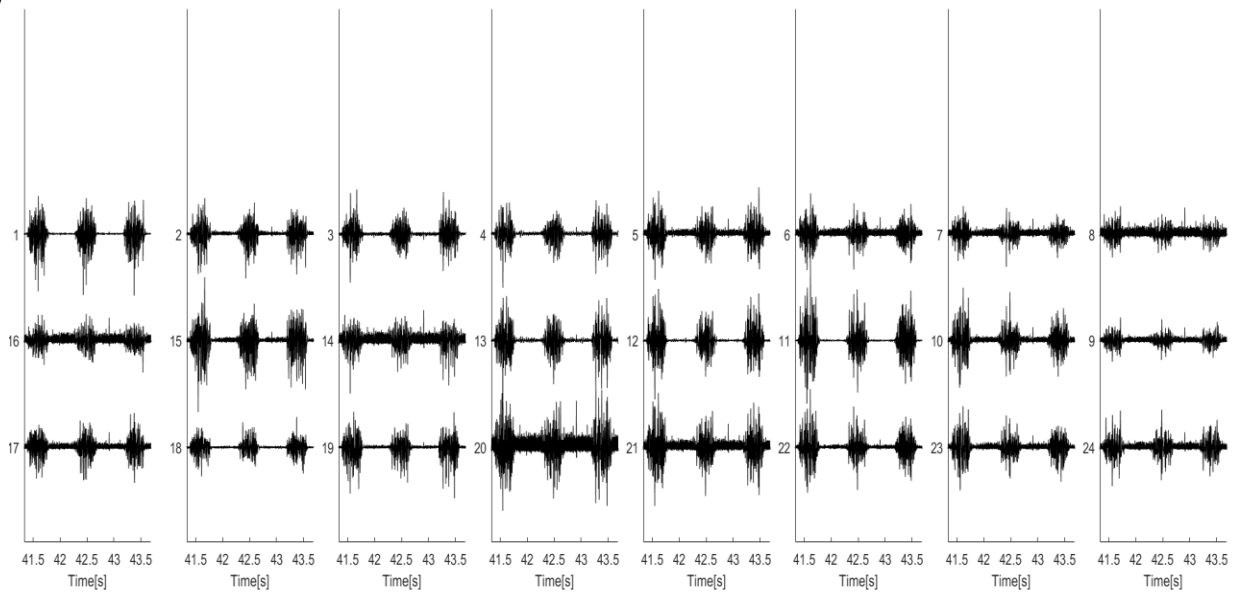


Figure 4.5.4: an example of single differential EMG coming from vastus medialis, proximal /region (a) and distal region (b) during preliminary tests; no difference in activation timing is noticeable within the same region. Therefore, a single bipolar electrodes couple to map their activity is acceptable.

Here there is a final table to recap all muscles which were involved in the experimental protocol and their associated detection systems:

Muscles	Detection system	Detection Device
Rectus femoris (proximal)	16x2, 1.5 cm IED array (electrodes 1-16)	Multichannel EMG detection device (Meacs)
Rectus femoris (distal)	16x2, 1.5 cm IED array (electrodes 17-32)	Multichannel EMG detection device (Meacs)
Vastus medialis (proximal)	Couple of disposable bipolar electrodes	Bipolar EMG detection device (DuePro®)
Vastus medialis (distal)	Couple of disposable bipolar electrodes	Bipolar EMG detection device (DuePro®)
Gastrocnemius Medialis	Couple of disposable bipolar electrodes	Bipolar EMG detection device (DuePro®)
Tibialis Anterior	Couple of disposable bipolar electrodes	Bipolar EMG detection device (DuePro®)
Biceps Femoris	Couple of disposable bipolar electrodes	Bipolar EMG detection device (DuePro®)
Gluteus Medius	Couple of disposable bipolar electrodes	Bipolar EMG detection device (DuePro®)
Soleus (medialis)	Couple of disposable bipolar electrodes	Bipolar EMG detection device (DuePro®)
Soleus (lateralis)	Couple of disposable bipolar electrodes	Bipolar EMG detection device (DuePro®)

Table 1: quick recap on involved muscles and used electrodes and devices for each of them

Please notice that these notations (medialis, lateralis, proximal, distal), with Gastrocnemius Medialis as the only exception, are only a convenient expression to use when referring to these muscles' portions, but they are not real anatomical/scientific expressions.

4.6 Chosen parameters for EMG and biomechanical signals elaboration and muscle synergies extraction

An overall description of NNMF algorithm is provided in Chapter 3.3. In this new chapter, all values of any involved parameters in these two phases of data elaboration are reported with a relative comment to justify their choice.

EMG and biomechanical signals elaboration (see Fig. 4.6.1 and Fig. 4.6.2)

- Raw EMG signals were bandpass filtered between 20 and 500 Hz, which is the frequency range where a consistent amount of EMG power spectrum density can be found; 20 Hz was chosen as the low cut-off frequency to reduce as much as possible presence of motion artefacts.
- Biomechanical signals from electrogoniometers, applied to subjects' knee during cycling tasks, were searched for their Bottom Dead End (i.e, lowest-tension points in the signal) and a complete cycle was defined by two consecutive BDE. On the other hand, two pressure sensors adopted as footswitches were positioned under subject's heel and third metatarsal head respectively. Only one sensor placed on the heel is sufficient to obtain a satisfying gait segmentation ^[20], although monitoring toes clearance with a second sensor is always recommendable. In this case, two consecutive heel strike would define a complete gait cycle.

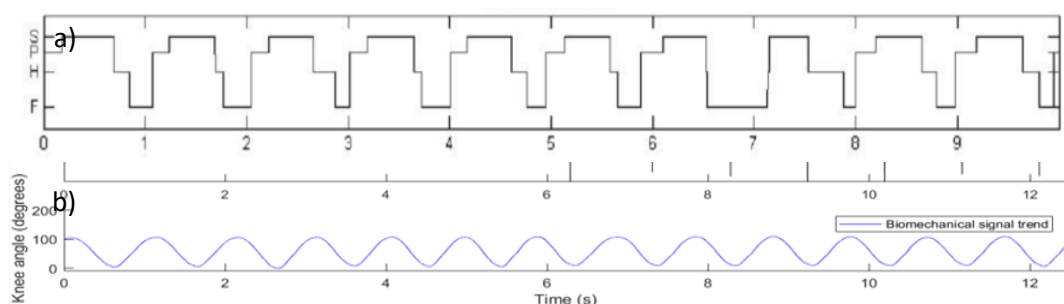


Figure 4.6.1: typical trends of signals from footswitches (a) or electrogoniometer (b)

- every walking/cycling complete cycle for each subject was investigated with respect to EMG quality and artefact absence, downsampled from their original length to 200 samples, then concatenated in a $n \times 200$ long array (Olivera et al. ^[18]), where n is the

number of cycles at disposal; however, any low quality cycle was not considered for any further analysis and it was eliminated from data structures. Concatenating consecutive task cycles is the best way to preserve EMG variability despite some quality loss in signal reconstruction^[18]. Due to the fact that this method is used much more frequently in literature rather than averaging EMG from different cycles, it was chosen to extract synergies.

- EMG concatenated cycles are rectified, then lowpass filtered with a Butterworth 2th-order filter, cut-off frequency at 10 Hz (Olivera et al.^[18]) to calculate EMG envelopes; while Barroso et al.^[20] worked with a 5 Hz cut-off frequency, M. van der Krogt et al.^[33] studied filtering effects on muscle synergies extraction and confirmed that for equal number of muscle synergies VAF values decrease at higher cut-off frequencies. This is reasonable since higher cut-off frequencies would tend to save EMG variability and cause envelopes to be less smooth, which also means they should be more difficult to reconstruct though. Nevertheless, a cut-off frequency of 10 Hz was considered more appropriate for the purpose of this thesis because, according to M. van der Krogt et al.^[33], extracted synergies should be totally confrontable with those obtained by Barroso et al.^[20]
- since this operation is repeated for all considered muscles, all EMG arrays for each muscle must be normalized by its respective max value in order not to bias NNMF results, otherwise a muscle whose EMG has a higher amplitude than others might be recognized as predominant in extracted muscle synergies.

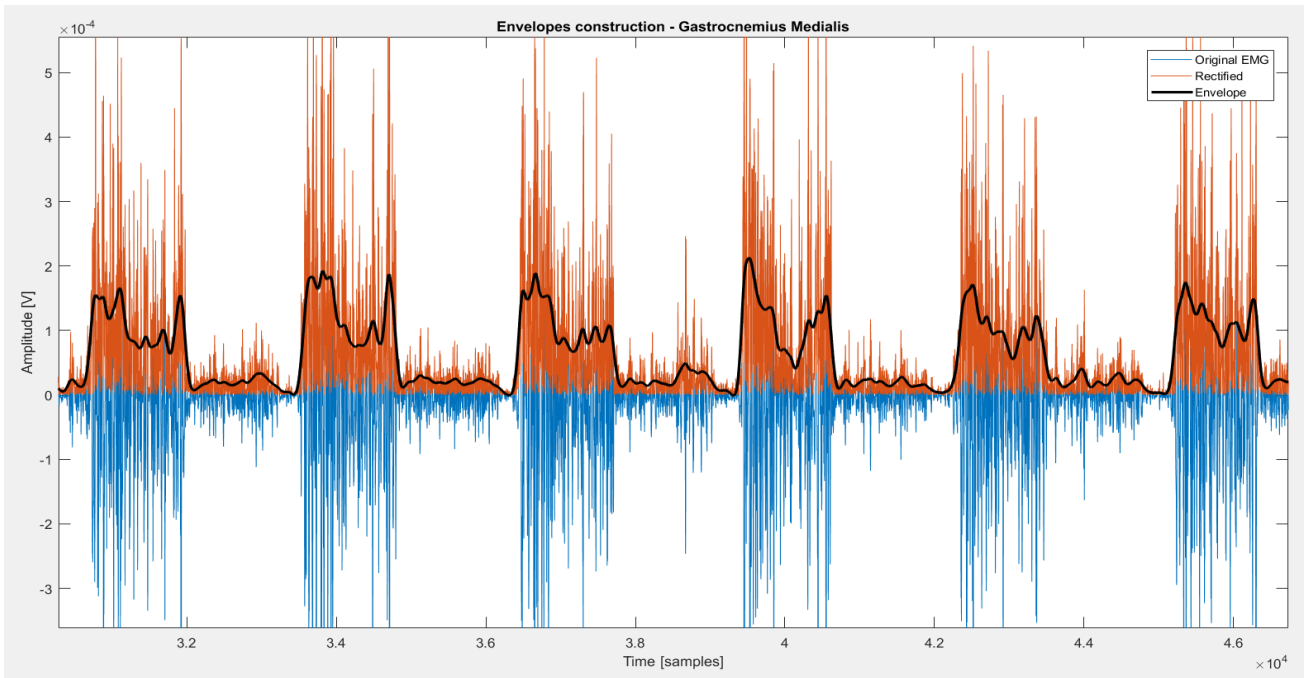


Figure 4.6.2: phases of EMG reconstruction; in this picture, original EMG (in blue), rectified original EMG (in red) and EMG envelopes (in black) are overlapped.

For each subject transversal single-differential signals (see chapter 4.7) from Rectus Femoris were calculated and therefore synergies were extracted for each task.

- NNMF algorithm
 - Max number of iterations to reach convergence per single extraction: 1000
 - Termination tolerance on change in size of the residual: 10^{-6}
 - Termination tolerance on relative change in the elements of W and H: 10^{-6}

Even though a few more minutes are required for the algorithm to reach convergence due to such parameters, it's safe to say that obtained results are totally stable and repeatable [28].

Moreover, as NNMF algorithm might be stuck in local minima despite reaching convergence, synergies extraction is repeated 40 times (Barroso et al. [20]) and the chosen final H and W

matrixes are those associated with the run with the lowest residual, which is formulated as follows:

$$D = \frac{A-W*H}{||A-W*H||} * \frac{1}{\sqrt{N*M}} ,$$

where A is the original EMG envelopes matrix, W and H are the synergies weights and temporal coefficients matrixes, N and M are matrix A's dimensions. As shown in Barroso et al. ^[20], Olivera et al. ^[18] and Clark et al. ^[25]'s work, VAF (see Chapter 3.3) adopted value was 0.90.

4.7 Post-processing and indicators for synergies comparison

Since muscle synergies are extracted directly from EMG envelopes, whose quality and effectiveness in replicating EMG original signals depends on a series of factors (cut-off frequency, filter order, motion artefacts and abrupt spikes, etc.), checking EMG quality first was key.

For each trail and analysed subject, EMG signals were always visualized both online on *bp*[®] and offline on *Matlab*[®] to ensure that no abnormal activity corrupted them during the acquisition.

An additional and final mention regarding rectus femoris must be made: 32 monopolar electrodes allow to simulate 31 different single-differential signals, each of them separated by 1.5 cm. Because of rectus femoris' structure, with long pennate fibers yet not very developed in depth, this interelectrode distance fits very well to investigate a very selective detection volume. However, since analysing both global proximal and distal activity is the ultimate goal, it was decided to sum all possible triplets of monopolar electrodes together (1-3-5, 2-4-6, etc.) from both columns of electrodes at disposal, then chose one proximal and one distal triplet of electrodes again for both column, calculate their respective transversal single differentials to obtain a signal describing EMG activity cumulatively in the proximal region and another one for the distal region. A graphical description of this process is shown in Fig. 4.7.1.

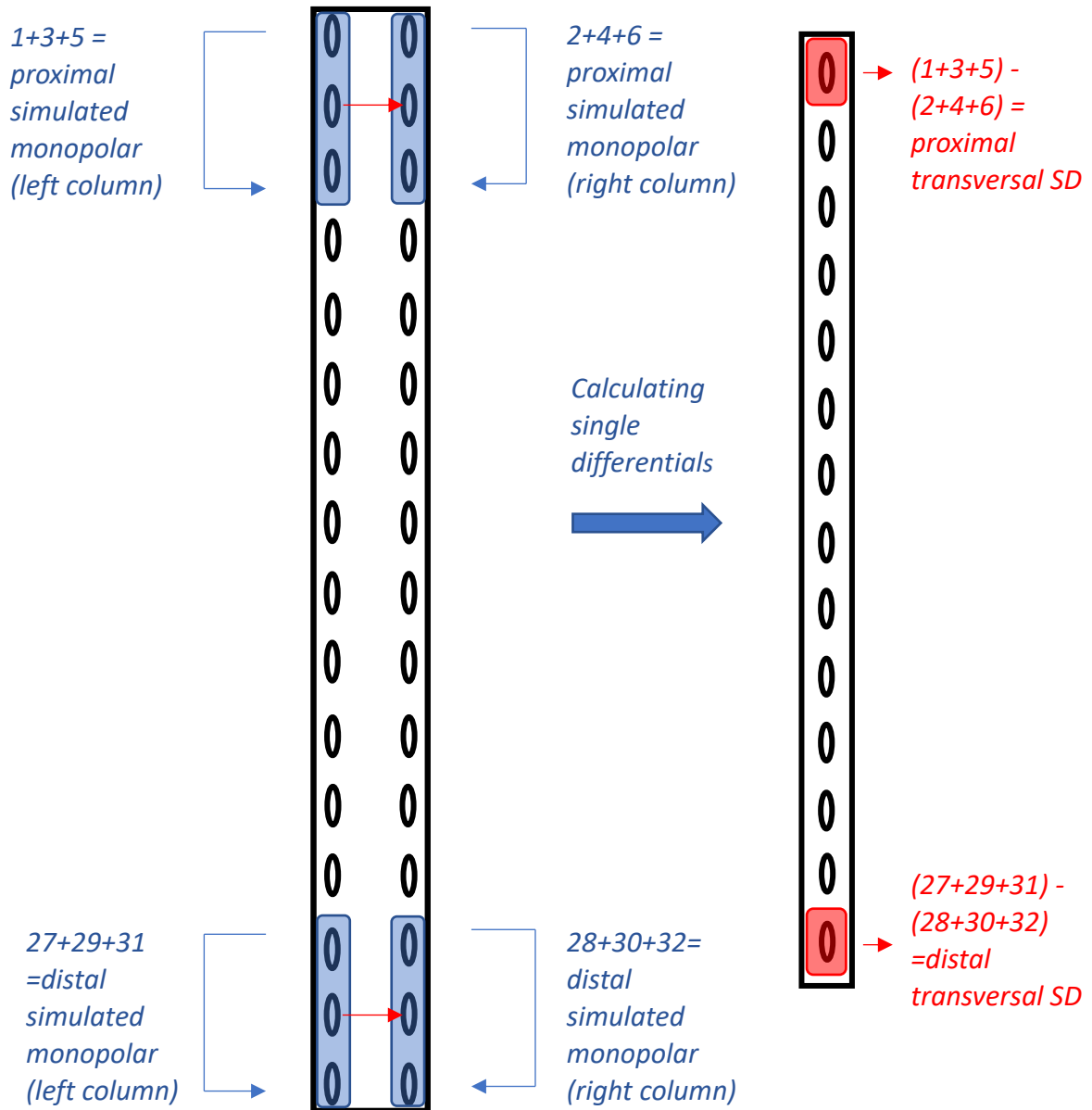


Figure 4.7.1: graphical explanation of how Rectus Femoris signals were elaborated; as shown in the picture, triplets of consecutive electrodes from each column were averaged together to simulate a larger detecting electrode, without losing spatial selectivity then by calculating transversal single-differentials.

Synergies were also analysed through Watanabe et al. [35] methods and signals from electrodes of the same row were first averaged, single differentials along the longitudinal direction were simulated and then synergies extraction was performed again. However, it must be pointed out that no significant change was observed in the so-calculated single differential signals.

Notice that, for gait analysis, U-turns were removed before initializing segmentation and every first and last step was also removed, since it's better to analyse steady steps, with no acceleration/deceleration induced from starting or finishing consecutive gait cycles. Then, 20 tasks cycles were chosen for each subject in order to make sure noise or artefacts couldn't significantly affect signal-noise ratio and to preserve natural EMG variability while still working with a reasonable amount of cycles [18].

After synergies extraction is completed for all subjects, two indicators were used to compare different activation coefficients and synergies weighting values and these are the max value of Zero-Lag Cross Correlation and Cosine Similarity respectively.

- Zero-Lag Cross Correlation

This parameter, whose values can span from -1 to 1, is an evaluation of how correlated (i.e. "similar") two different activation coefficients are. Zero-Lag Cross Correlation is formulated as follows:

$$CC = \frac{R_{xy}[0]}{\sqrt{R_{xx}[0] * R_{yy}[0]}}$$

where R_{xy} is the cross-correlation function, R_{xx} is the autocorrelation function for the first activation coefficient and R_{yy} is the autocorrelation for the second activation coefficient.

$$R_{xy} = \int_{-\infty}^{+\infty} x(t)^* y(t + \tau) dt$$

This parameter has been calculated by Matlab function *xcorr* (option 'coeff').

- Cosine similarity

Weight values' repeatability and similarity are checked through Cosine Similarity, which confronts two weight vectors from two different synergies by calculating their normalized scalar product:

$$CS = \frac{W_i * W_j}{\|W_i\| * \|W_j\|}$$

Each synergy from different subjects, after having ordered possibly matching activation patterns through Zero-Lag Cross Correlation, was evaluated in terms of weights similarity to check if the same involved muscles happen to have similar global activation levels as well. CS equal to 0 means that the two weights vectors have no resemblance at all, while CS=1 indicates full similarity.

As NMF algorithm provides with synergies whose activation coefficients and weighting values are extracted randomly each time, these two parameters are especially important to overlap similar synergies from different subjects when they are plotted and check intra-subject variability as well as among synergies from the same subject.

5. Results

5.1 Envelopes from Rectus Femoris during Gait: preliminary comparison with Watanabe et al. [35]' study

Watanabe et al. [35] carried out a specific study about rectus femoris' activity during treadmill gait in order to assess region-specific differences between proximal and distal ends of the muscle. First, they calculated RMS values for each 2% of every stride length and across 20 strides for each subject, then they averaged all obtained results among all subjects and all task conditions. As it can be seen from Fig. 5.1.1, rectus femoris' behaviour as a biarticular muscle is clear: considering heel strike as the initial phase of each cycle, at 10% and 90% of task duration rectus femoris' distal region takes a more significant part in knee extension than its proximal region, while the latter is also activated around 60% of gait cycle during toe-off phase and participates more importantly in hip flexion.

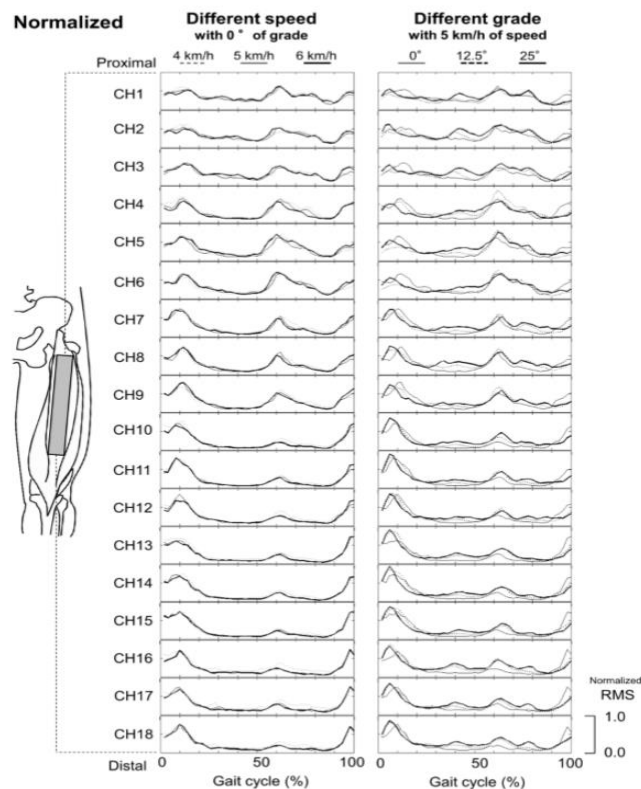
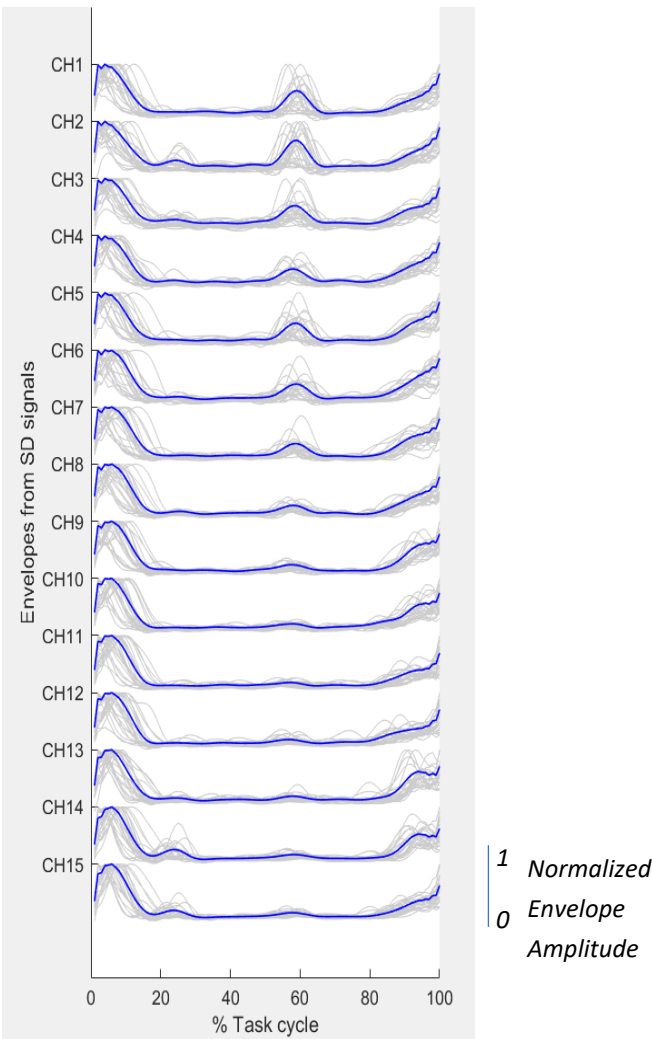


Figure 5.1.1: Watanabe et al. [35]'s analysis of rectus femoris' activity during gait: distal portion of rectus femoris appears to be majorly involved both at the beginning and at the end of gait cycle, when knee extension is performed; on the other hand, the proximal end seems to be more active during hip flexion, which occurs just before the beginning of swing phase; notice that these RMS normalized values were averaged among all studied subjects and gait conditions.

In the present study, this behaviour was found as well (Figure 5.1.2), but in 3 subjects out of 8 only, while all remaining 5 showed little if not any relevant differences between proximal and distal rectus femoris' regions (Figure 5.1.2a). As stated in Chapter 4.7, single differentials were calculated both longitudinally and transversally to explore EMG propagation in the best possible way. Fig. 5.1.2b represents the transversal single differential signals from the same subject whose rectus femoris' activation patterns were illustrated in Fig. 5.1.2.

a) Longitudinal Single Differential – IED 1.5



b) Transversal Single Differential – IED 3 cm

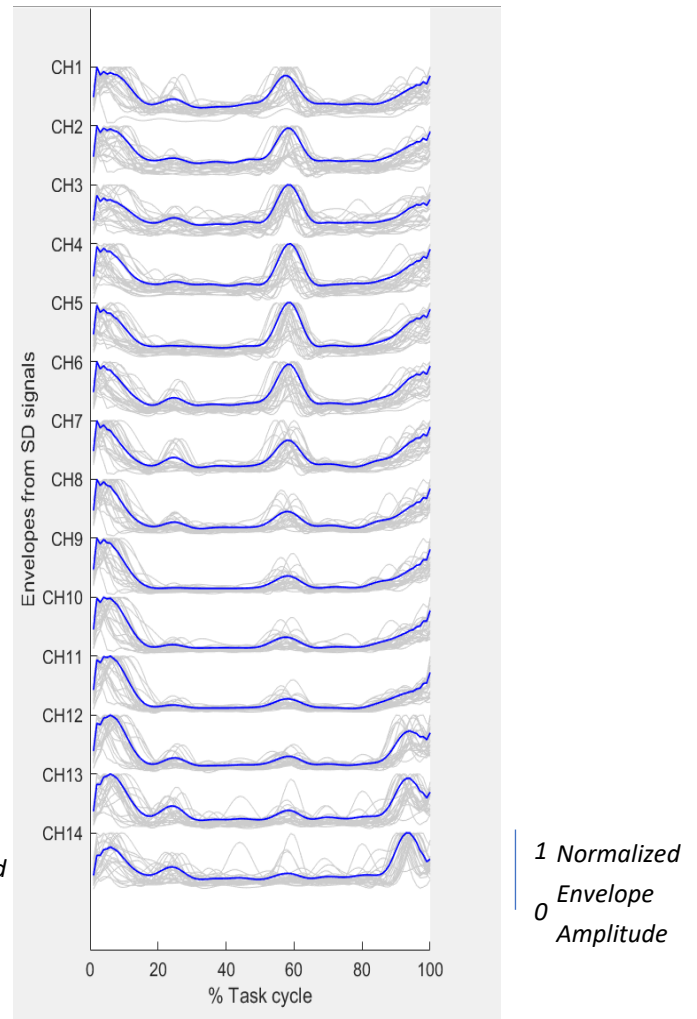


Figure 5.1.2: a) typical behaviour of those subjects who have shown differences in RF regions' activities; these activation patterns were found in 3 subjects out of 8 only

Figure 5.1.2 b): transversal single-differentials from rectus femoris from the same subject whose RF's activity was shown in figure 5.1.2; transversal and single-differential signals seem

to be very repeatable and comparable, which would lead to basically equal results from synergies extraction outcome. Due to this main reason, after a few tests which confirmed this hypothesis, synergies extraction was performed with longitudinal single differentials only.

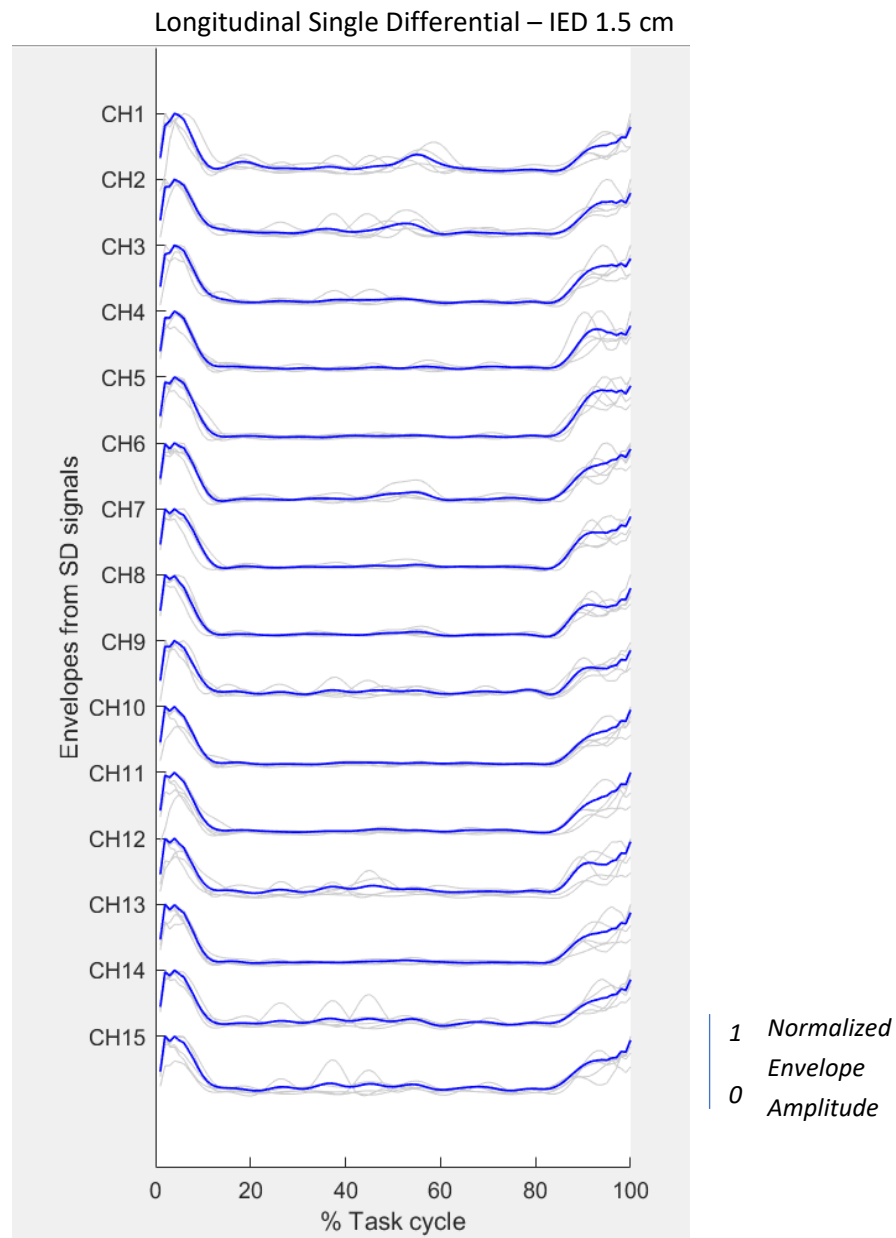


Figure 5.1.3: example of rectus femoris activity in those subjects who showed little or even no differences in RF regions' activities

it's quite clear how transversal and longitudinal single differentials are very much alike, which made no significant difference in muscle synergies extraction outcome in fact. Therefore, since no particular evidence about transversal single differentials providing with extra information regarding rectus femoris' behaviour, it was decided to report results obtained by extracting synergies from longitudinal single differentials only.

5.2 Muscle synergies extraction results - Gait

Synergies extraction from gait was performed on 6 out of 8 analyzed subjects, due to motion artifacts and noise corrupting most of Vastus Medialis' EMG signals for both excluded subjects. Adopted VAF was 0.90 and this resulted in 4 synergies for each subject (Fig. 5.2.1 and Fig. 5.2.2).

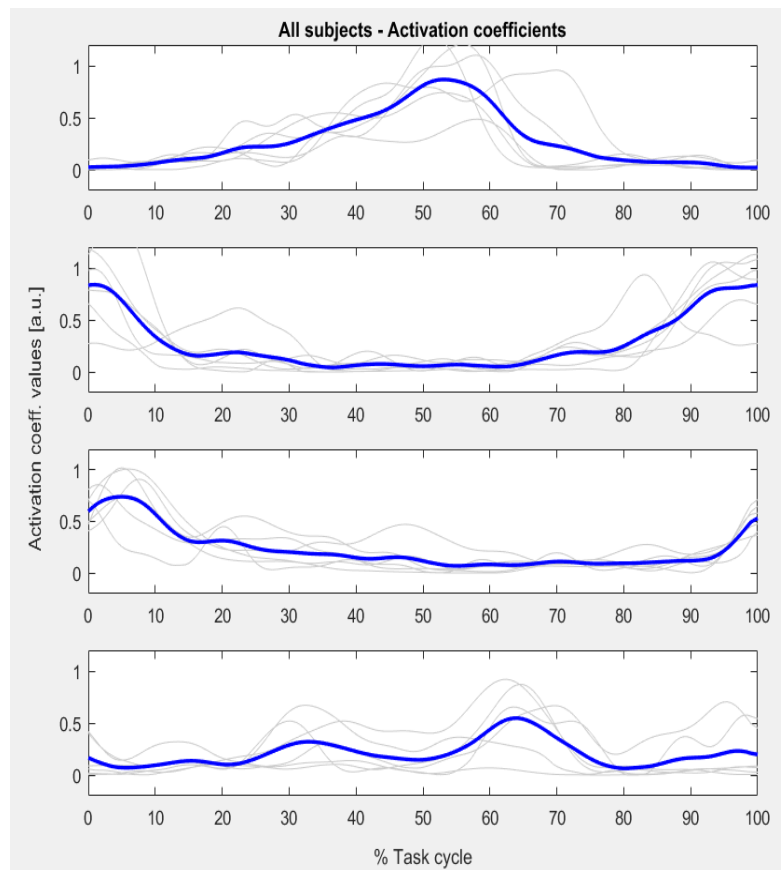


Figure 5.2.1: all synergies extracted from 6 subjects during gait (2 of the initially analyzed 8 subjects were excluded due to motion artifacts and non-physiological spikes affecting EMG quality in Vastus Medialis); thicker blue line represent an average trend for each activation coefficient among all subjects. Task cycle duration is normalized to its own length and then expressed as percentage, where 0% and 100% represent two consecutive heel-strikes.

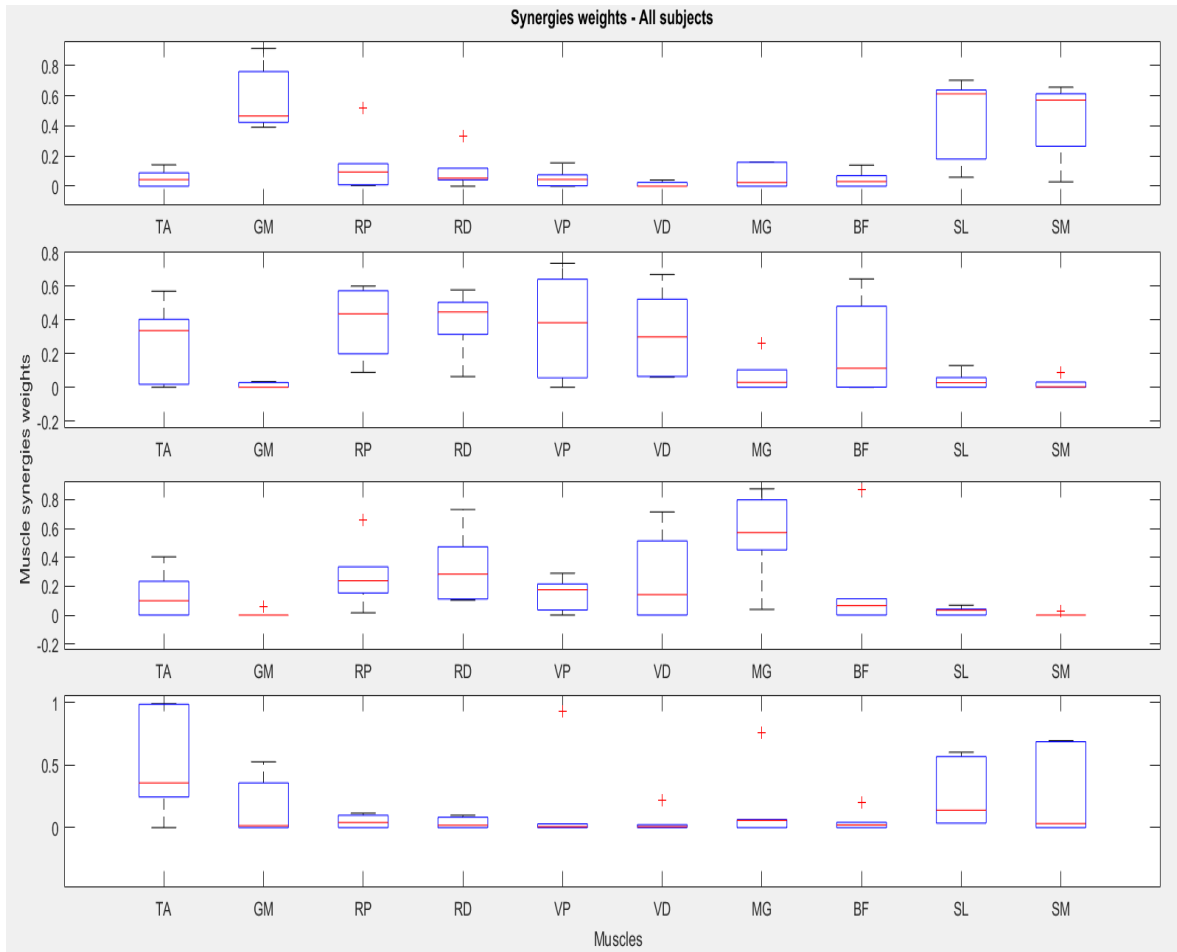


Figure 5.2.2: all synergies extracted from 6 subjects during gait (2 of the initially analyzed 8 subjects were excluded due to motion artifacts and non-physiological spikes affecting EMG quality in Vastus Medialis); weights values are reported here in boxplots, where the red line is the median value (calculated across all subjects) for each muscle' weight values associated with each synergy . Boxplot window boundaries represent 25th percentile and 75th percentile respectively, while red crosses are values recognised as outliers.

If compared with previous works found in literature ^{[20][25]}, muscle synergies obtained during gait show both common and peculiar behaviours: as described in Chapter 3.4, synergy 1 from picture 5.2.1 and 5.2.2 clearly represents Medial Gastrocnemius and Soleus muscles activity during pre-swing, widely documented in all studied muscle synergies extraction work. Synergies 2 is a combination of late swing phase, in which Biceps Femoris is the principal active muscle (Semitendinosus is also another important actuator during late swing, but it wasn't analyzed in this study) and contributions from Tibialis Anterior, Vastus Medialis and

Rectus Femoris during midstance phase and at initial swing phase. Synergy 3 describes cumulative activations from Tibialis Anterior and Medius Gluteus, which are involved during heel-strike and foot-flat stance, as well as Vastus Medialis. Synergy 4 describes localized activation patterns from Tibialis Anterior, Medial Gastrocnemius and both portions of the Soleus muscle.

Comparing median values and overall trends of muscle synergies weights for Rectus Femoris, Vastus Medialis and Soleus' regions, there seems to be no evident overall distinction within each muscle in terms of contributions to a specific synergy. Further investigation was then carried out to assess if any possible difference stands out at least in some subjects. Therefore, it was chosen to extract muscle synergies from all 6 subjects once again, but this time extraction was repeated twice, first excluding Rectus Femoris' proximal envelopes and then Rectus Femoris' distal envelopes. The purpose of this new test was to check similarity between extracted synergies from each subject considering only one of the two investigated Rectus Femoris' portions at a time. The outcome of this test for one subject is represented in Fig. 5.2.3 and Fig. 5.2.4 as an example.

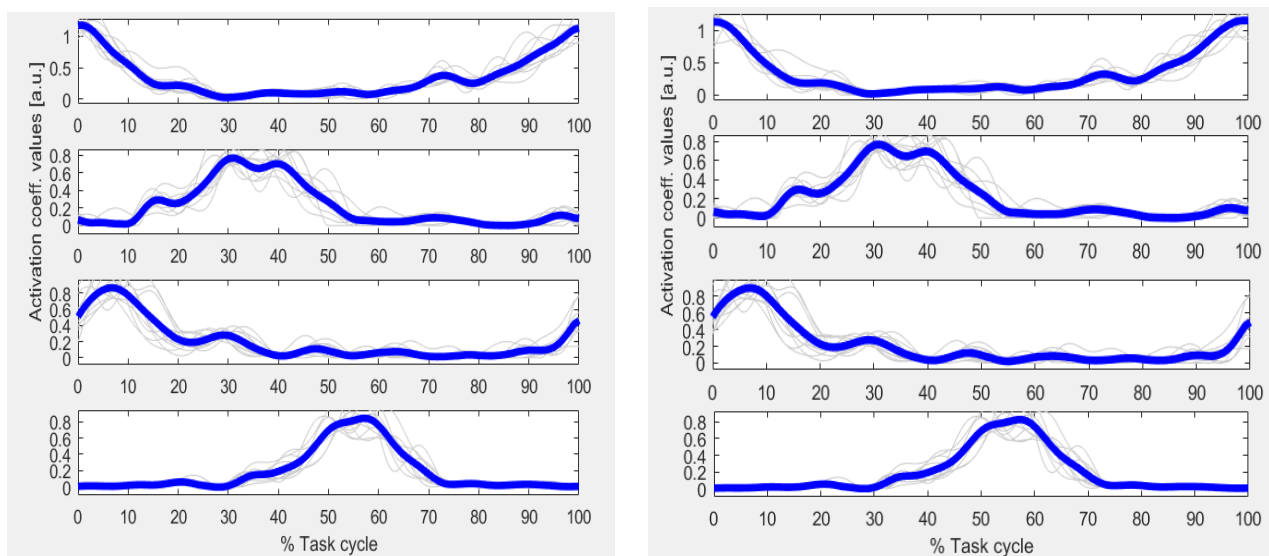


Figure 5.2.3: on the left, activation coefficients from subject 1' muscle synergies during gait are plotted; synergies were extracted without distal Rectus Femoris' contributions. On the right, activation coefficients from synergies without proximal Rectus Femoris' contributions from the same subject are presented instead.

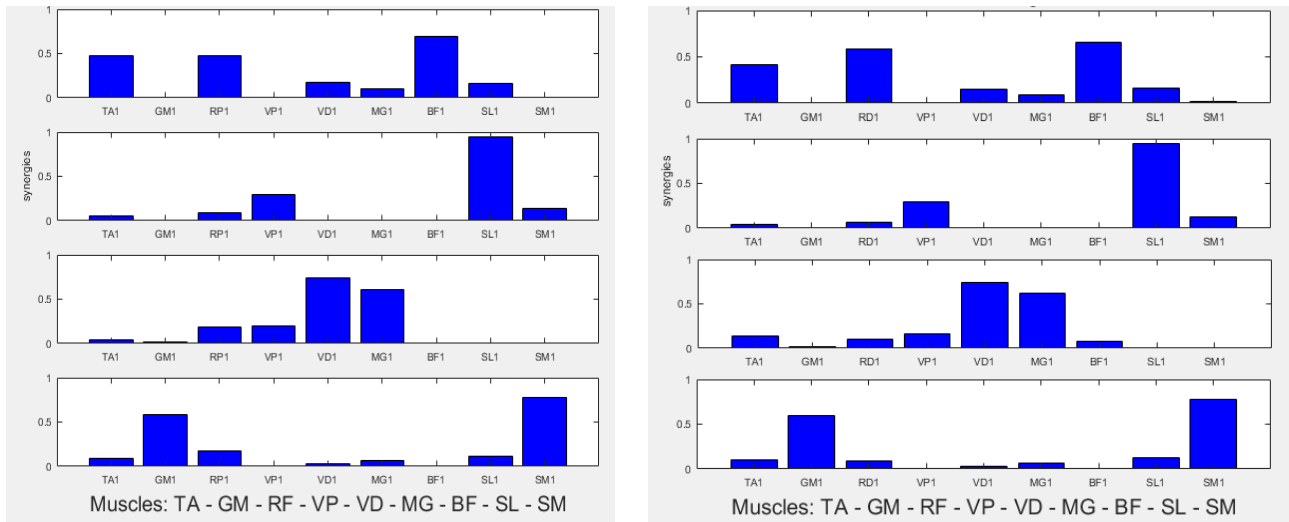


Figure 5.2.4: on the left, weight values from subject 1' muscle synergies during gait are plotted; synergies were extracted without distal Rectus Femoris' contributions. On the right, weight values from synergies without proximal Rectus Femoris' contributions from the same subject are presented instead.

Cosine similarity (see Chapter 4.7) was chosen to evaluate similarity between each couple of weight vectors from the two conditions of extraction.

Subjects	CS Synergy 1	CS Synergy 2	CS Synergy 3	CS Synergy 4
s1	0.9835	0.9969	0.9924	0.9908
s2	0.9928	0.9884	0.9940	0.9895
s3	0.9790	0.7451	0.9937	0.6429
s4	0.9965	0.9983	0.9867	0.9706
s5	0.9986	0.9974	0.9999	0.9997
s6	0.9991	0.9901	0.9998	0.9944

Table 2 – Cosine Similarity (CS) values to assess possible differences in muscle synergies extracted during gait excluding RF proximal and distal alternatively

As highlighted in yellow (see Table 2 above), in only one case Cosine Similarity was not above 0.9 (a threshold commonly used in literature ^[7]) and that is subject 3. This subject was also one of those three subjects who reported some degrees of difference between proximal and

distal regions of Rectus Femoris' activity. Muscle synergies extracted during his gait task are reported below (Fig. 5.2.5):

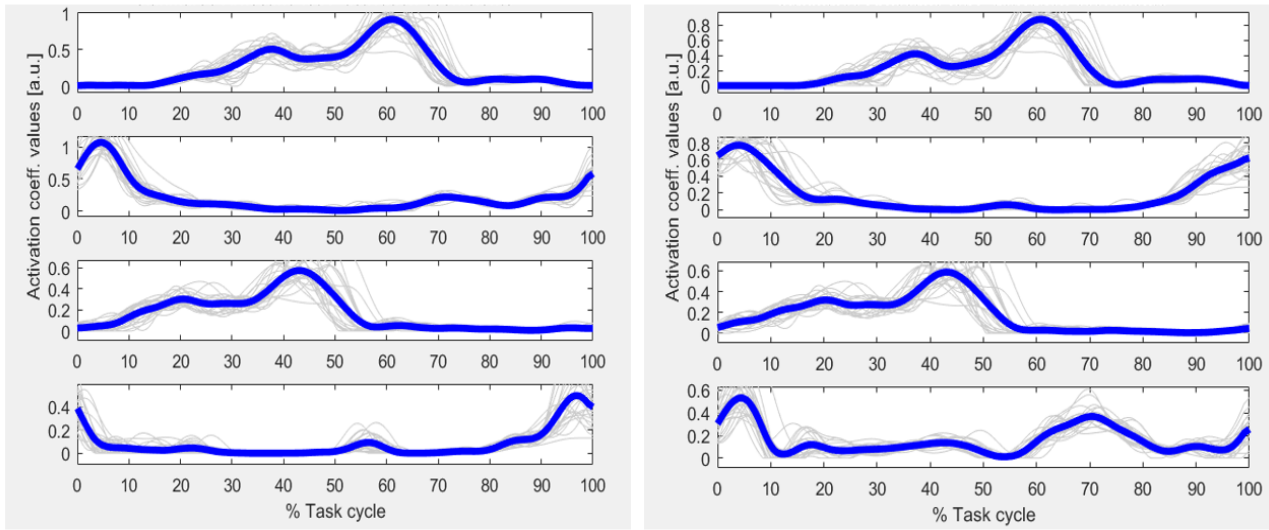


Figure 5.2.5: activation coefficients extracted from subject 3, who was the only one to reveal significant differences between synergies extracted considering only RF proximal and distal regions alternatively. The last activation coefficients are visibly different from each other, which can be noticed in synergies weight values as well (Fig 5.2.6).

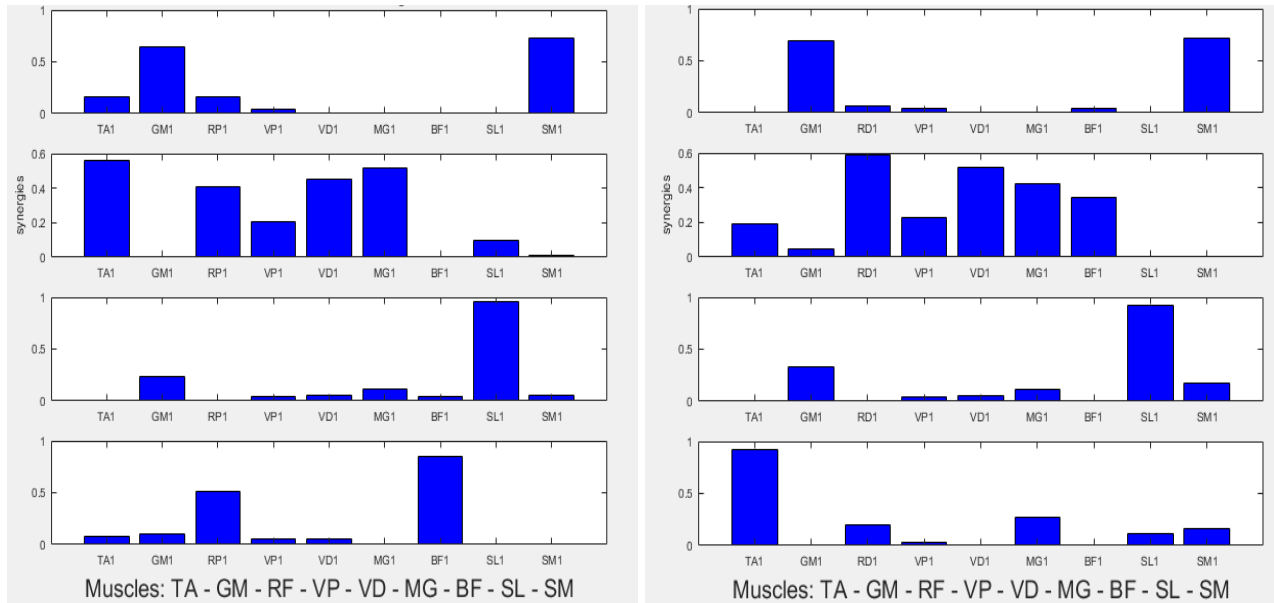


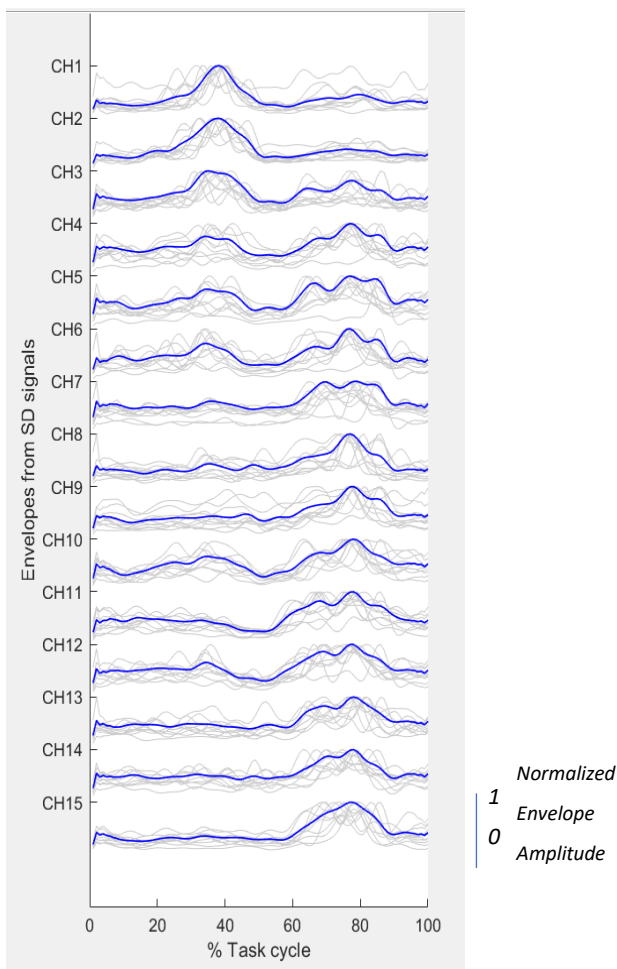
Figure 5.2.6: weight values extracted from subject 3, who was the only one to reveal significant differences between synergies extracted considering only RF proximal and distal regions alternatively.

From Fig. 5.2.6, it stands out how different muscle weight distributions are between synergies 2 and 4 especially. For subject 1 and 4, who also revealed different behaviours within the two regions, no significantly lower CS values were obtained instead.

5.3 Envelopes from Rectus Femoris in Cycling

Since this study's aim is to understand how region-specific muscle activations might be an influent factor on muscle synergies extraction outcome in cycling analysis too, envelopes from Rectus Femoris extracted from subjects during cycling are reported below (both transversal and longitudinal): activation patterns in Fig. 5.3.1 were common among all subjects and they also match with preliminary study results shown in Chapter 4.5, where rectus femoris' proximal and distal regions appeared to be activated in separate task phases.

Longitudinal Single Differential – IED 1.5 cm



Transversal Single Differential – IED 3 cm

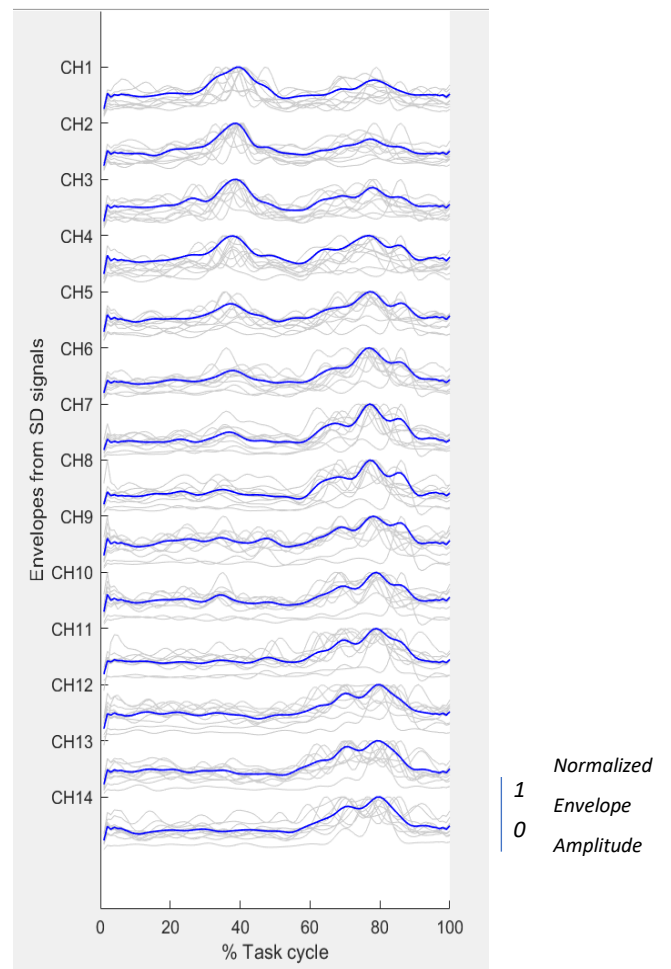


Figure 5.3.1: an example of rectus femoris' EMG envelopes during cycling from single differential signals, both longitudinal and transversal; assuming BDE (Bottom Dead End) as the start of each cycle, rectus femoris' proximal end is highly involved during the recovery phase while hip flexion occurs, while its distal end is far more active during power phase.

It must be pointed out, however, that this activation peak, progressively shifted towards more distal channels during late cycle phases, is not always so well defined in all subjects. Frequently, activation patterns in Rectus Femoris would appear as reported in Fig. 5.3.2.

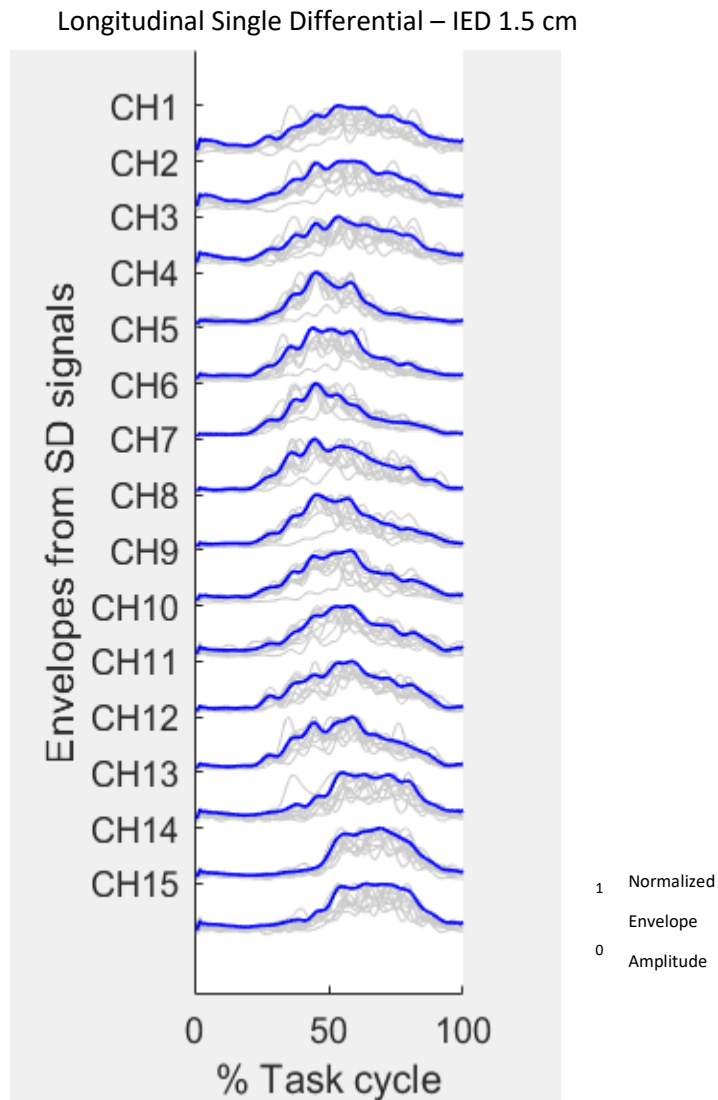


Figure 5.3.2: another example of rectus femoris' EMG envelopes during cycling; assuming BDE (Bottom Dead End) as the start of each cycle, rectus femoris' proximal end is highly involved during the recovery phase while hip flexion occurs, while its distal end is far more active during power phase. However, differences between distal and proximal regions are not so clear anymore as in Fig. 5.3.1.

Since this second activation pattern scheme is found more frequently among our subjects, muscle synergies might be less likely to be influenced by such differences in Rectus Femoris' activations.

5.4 Muscle synergies extraction results - Cycling

Synergies extraction was performed for cycling as well and 3 synergies were found for all subjects. The same 2 subjects which were excluded from gait synergies analysis are again not taken into account in cycling muscle synergies extraction due to artifacts corrupting Vastus Medialis' EMG. Therefore, only 6 out of 8 subjects' synergies were considered in this analysis.

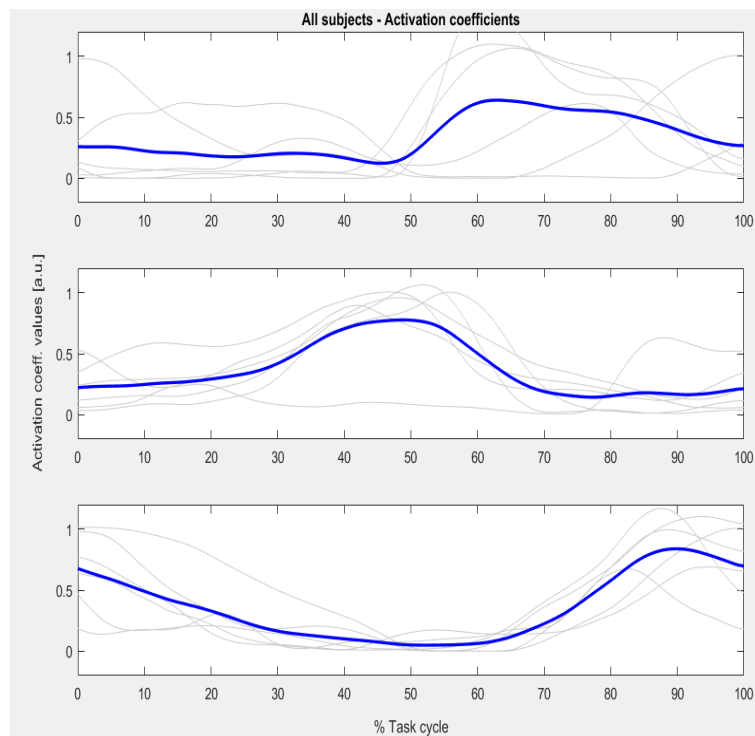


Figure 5.4.1: all synergies extracted from 6 subjects during cycling (2 of the initially analyzed 8 subjects were excluded due to motion artifacts and non-physiological spikes affecting EMG quality in Vastus Medialis); thicker blue line represent an average trend for each activation coefficient among all subjects. Task cycle duration is normalized to its own length and then expressed as percentage, where 0% and 100% represent two consecutive Bottom Dead End (which indicates complete knee extension).

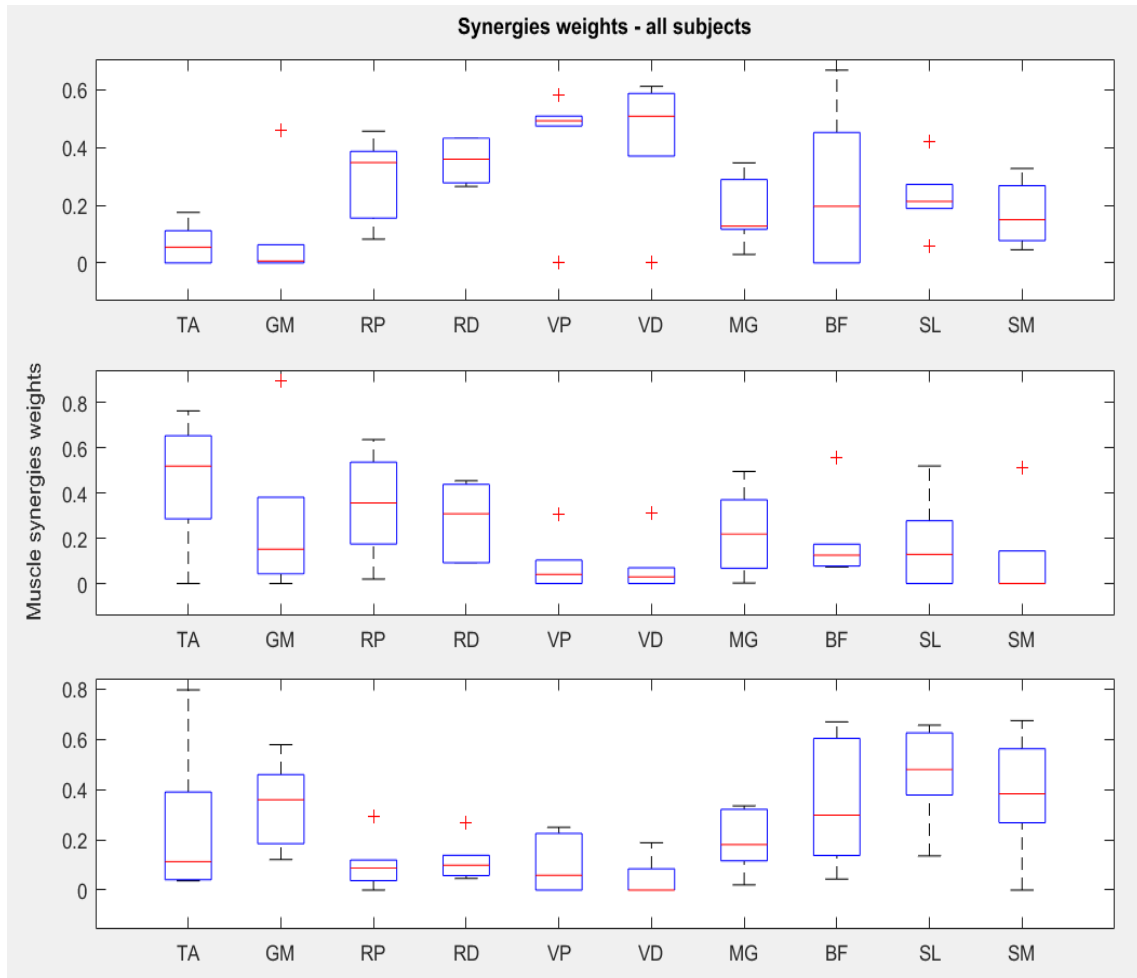


Figure 5.4.2: all synergies extracted from 6 subjects during cycling (2 of the initially analyzed 8 subjects were excluded due to motion artifacts and non-physiological spikes affecting EMG quality in Vastus Medialis); weights values are reported here in boxplots, where the red line is the median value (calculated across all subjects) for each muscle' weight values associated with each synergy . Boxplot window boundaries represent 25th percentile and 75th percentile respectively, while red crosses are values recognised as outliers.

Synergy 1 is also found by Barroso et al. ^[20], whose work highlights Biceps Femoris, Gluteus Medius and Soleus' activations during power phase (>50% task cycle); however, the present study also shows non-negligible contributions from Rectus Femoris and Vastus Medialis for this synergy. Synergy 2 is comparable to the one reported by Barroso et al. ^[20], since Vastus Lateralis, Rectus Femoris and Medius Gluteus are the main active muscles, even though Vastus Medialis' weight values appear significantly lower than what is suggested in their work. Synergy 3 combines activity from both recovery and power phases, with specific

emphasis on Tibialis Anterior, Medial Gastrocnemius and Soleus, while Rectus Femoris appears to provide with smaller contributions to this particular synergy.

After having extracted synergies from all 6 subjects, it was noticeable how two subjects assumed very different behaviours if compared to others. This is particularly clear in the first and second synergies, where two activation coefficients can't be comparable to the other 4. Due to this reason, excluding these two subjects from this analysis, a new set of muscle synergies was extracted (Fig. 5.4.3 and 5.4.4):

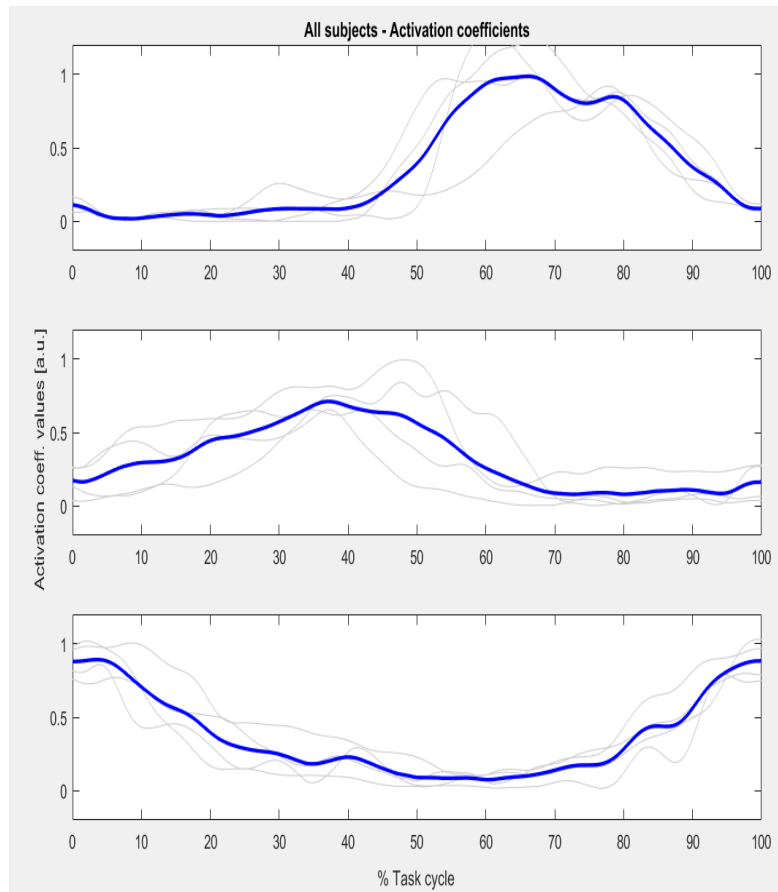


Figure 5.4.3: new set of extracted muscle synergies excluding two subjects who were significantly different from others; here, new activation coefficients are plotted. Thicker blue line represents an average trend for each activation coefficient among all subjects.

This choice of excluding two subjects from our analysis was made also because weight values could be affected by these two uncommon behaviours, which raises inter-subject variability in muscle synergies extraction outcome. New weight values are represented in boxplots for every muscle and synergy in Fig. 5.4.4:

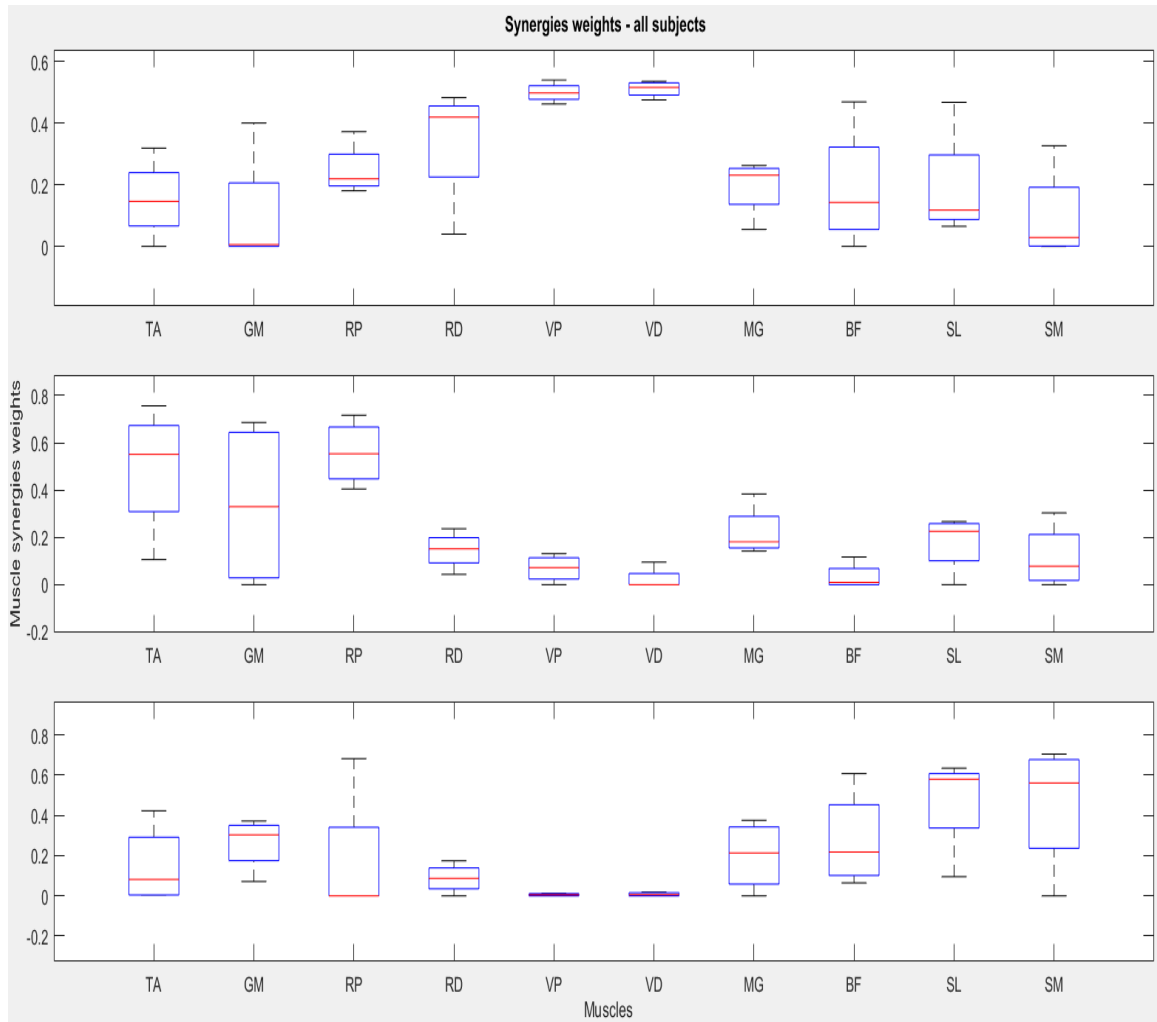


Figure 5.4.4: new set of extracted muscle synergies excluding two subjects who were significantly different from others; here, new weight values are plotted.

Interestingly, rectus femoris' proximal and distal regions seem to be clearly separated in the second synergy among the 4 remaining studied subjects. If compared to bike, a wider separation between the two regions' associated weight values (concerning at least median values) can be also seen in synergy 1.

As it was done for gait muscle synergies, synergies were calculated again separating rectus femoris regions in order to evaluate possible differences.

Subjects	CS Synergy 1	CS Synergy 2	CS Synergy 3
s1	0.9397	0.2697	0.7776
s2	0.9881	0.9538	0.9838
s3	0.9995	0.9871	0.9883
s4	0.9963	0.9995	0.9534

Table 3 – Cosine Similarity (CS) values to assess possible differences in muscle synergies extracted during bike excluding RF proximal and distal alternatively

As it can be noticed, even if the second synergy shows a significant difference in weight values between rectus femoris' proximal and distal regions, only one subject out of 4 actually induces a change in muscle synergies extraction results if the two regions are separated. Extracted synergies for this specific subject are shown in Fig. 5.4.5 and 5.4.6:

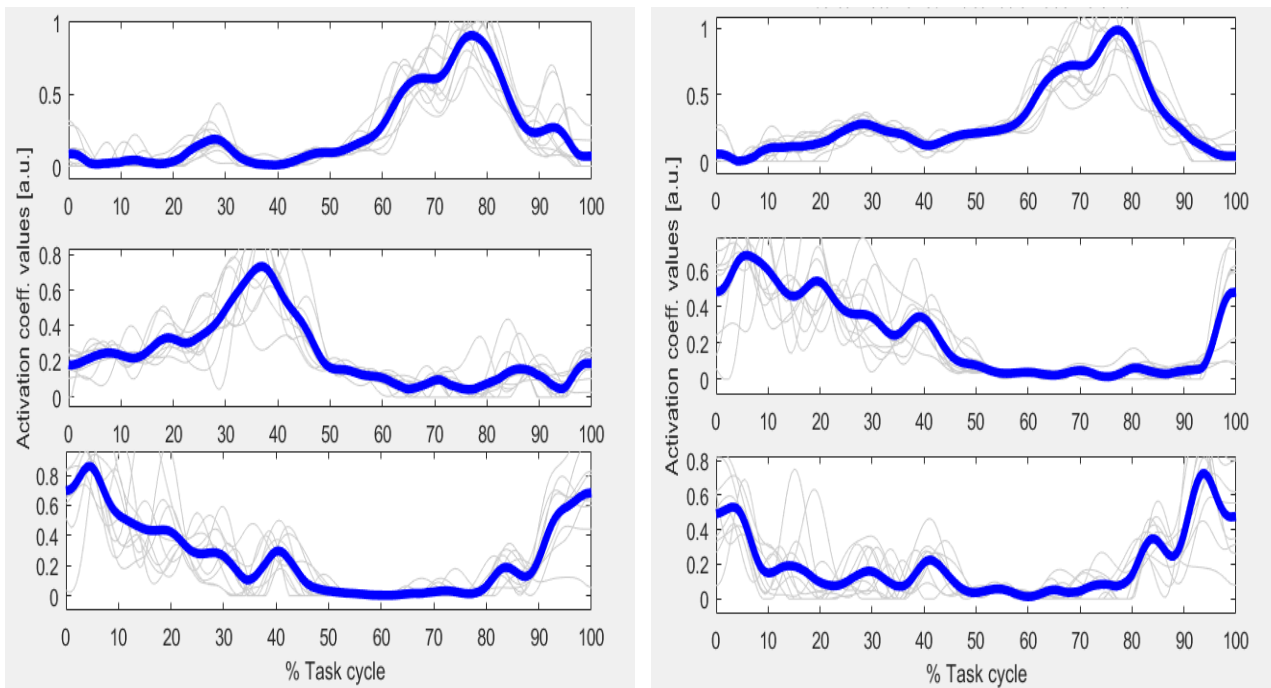


Figure 5.4.5: activation coefficients extracted from subject 1 first using Rectus Femoris' proximal (left) and distal (right) region separately

The third and especially the second synergies undergo a remarkable change considering only one Rectus Femoris' portion per extraction. The second activation coefficient progressively increases its amplitude at the beginning of gait cycle if proximal Rectus Femoris is considered, while it shows a rather opposite trend when distal Rectus Femoris is chosen. These changes are even more clear if weight values are taken into consideration.

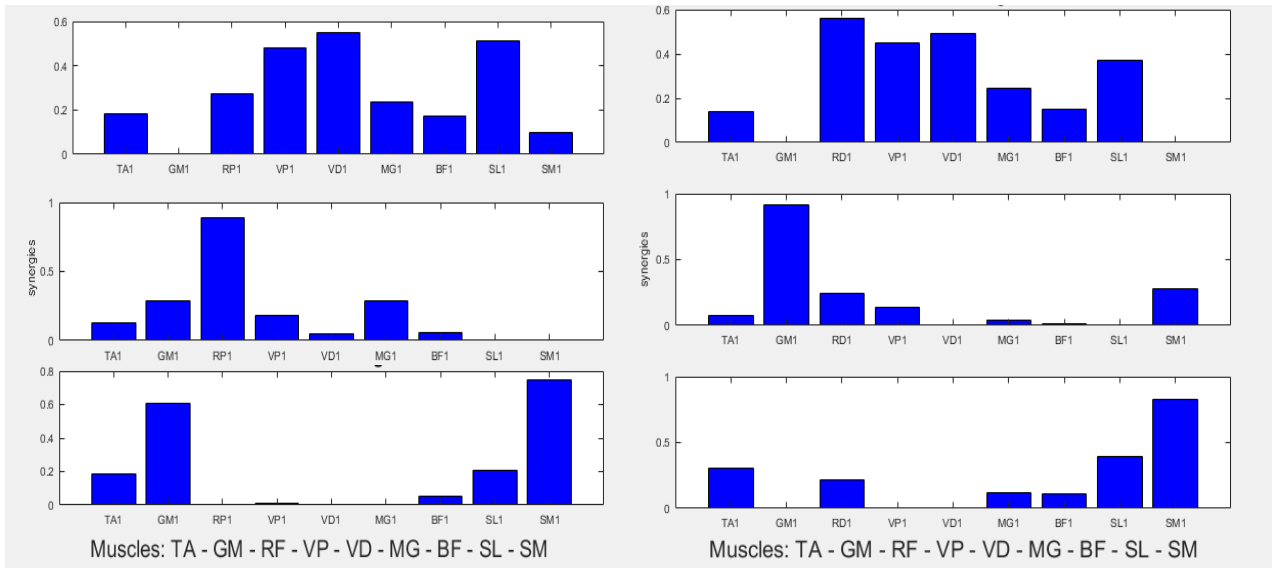


Figure 5.4.6: weight values extracted from subject 1 first using Rectus Femoris' proximal (left) and distal (right) region separately

In this subject's weight values, proximal Rectus Femoris is mainly active during the recovery phase, as suggested by the second synergy, while distal Rectus Femoris' weight value is higher during power phase (described by the first synergy) and it also appears in the third synergy, even if its presence is marginal.

However, this is only an isolated case, since other subjects do not reveal any particular difference in extracted synergies.

5.5 Results discussion

The present study investigated possible effects of region-specific functional roles within lower limb muscles on muscle synergies extraction. The main findings of this study are that no significant effect of inner region-specific functional roles of Rectus Femoris in particular, Vastus Medialis and Soleus.

First of all, EMG envelopes extracted from Rectus Femoris were comparable only in few cases with Watanabe et al. ^[35]'s results. This might be partially attributed to differences in methodological approaches between this present study and Watanabe et al. ^[35]'s: subjects were instructed to perform gait on a treadmill at pre-defined speed, while according to the experimental protocol adopted in this work it was decided to let them free to move and select their own pace. As shown by P.O. Riley et al. ^[36], slight differences in biomechanics between over-ground and treadmill are to be considered and even muscle synergies extracted from the two conditions show minor differences ^[26]. Even if they're not substantial changes, it was documented by S. A. Kautz et al. ^[26] that stride length decreased and stance percentage in gait cycle duration increased. Moreover, Watanabe et al. ^[35]'s findings suggest that proximal and distal differences in Rectus Femoris activation patterns are clearer at higher gait speed. The lowest tested speed in their work was 4 km/h, which is still higher than most of studied subjects' speed in this study. Due to the number of used probes and electrodes applied on each subject, walking at faster pacer could have been unconsciously avoided by some subjects in order to prevent some probes from falling and or some discomfort in the set-up could have caused them to decrease gait speed.

Nevertheless, some subjects still showed distinct activations between Rectus Femoris proximal and distal ends, particularly during cycling analysis. As reported, one synergy in particular showed well-separated behaviours between Rectus Femoris regions, which however weren't noticeable in muscle synergies extracted by separating the two portions. A first explanation could probably be associated with normalizing EMG envelopes to each muscle' maximum peak activity: small differences in Rectus Femoris proximal region (Fig. 5.1.2a) could be drastically reduced in size due to lateral peaks in the envelopes. Therefore, it's very likely to lose those details of activation. Fig. 5.4.4 shows us a seemingly consistent

difference between Rectus Femoris weight values in the second synergy, however this doesn't necessarily mean that the same difference is going to be spotted through Cosine Similarity values. If all other synergy weights are comparable, chances are that CS will still be high even if essentially only one muscle has different involvement in that particular synergy. Moreover, even if all subjects do present that specific feature, all other muscles might combine together in a way which may not allow it to be evident in extracted synergies. As further explanation of this concept, Fig. 5.5.1 shows envelopes signal reconstruction performed through linear recombination of matrix H and W (as illustrated in Chapter 3.3).

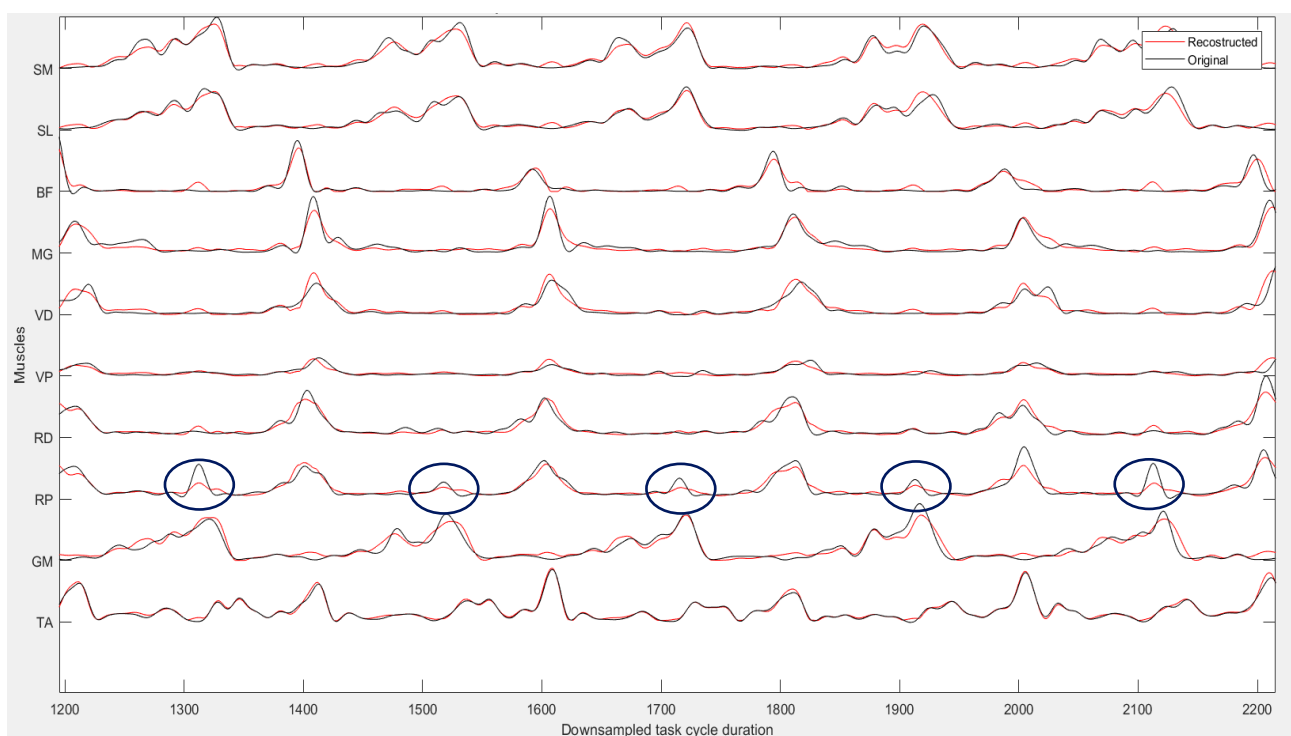


Figure 5.5.1: envelopes reconstruction results from extracted muscle synergies; reconstructed envelopes (in red) are overlapped on the original envelopes (in black); muscles abbreviations are TA (Tibialis Anterior), GM (Medial Gastrocnemius), Rectus femoris - Proximal portion (RP), Rectus femoris – Distal portion (RD), Vastus Medialis – Proximal portion (VP), Vastus Medialis – Distal portion (VD), Gluteus Medius (MG), Biceps Femoris (BF), Soleus Lateralis (SL) and Soleus Medialis (SM). Here we can observe 5 steps in a row (each of their durations was down-sampled to 200 samples). Blue circles highlight how activations in Rectus Femoris' proximal portion at about 50% of gait duration are not precisely reconstructed and are likely to be underestimated.

In Fig 5.5.1, it can be noticed how small details (even with a 90% VAF adopted ad threshold) are not well reconstructed and central proximal activity in Rectus Femoris is usually downsized. In order to make it more clear, a higher VAF would probably be required, but in that case the number of extracted synergies would increase as well.

Finally, since a limited pool of subjects was analyzed, further investigation on a larger number of subjects should be required to further confirm suggested statements in the present chapter.

6. Conclusions

The aim of this study was to analyze effects of region-specific functional roles in lower limb muscles muscle on muscle synergies extraction.

Carried out simulations and tests suggest that no relevant statistical evidence support the presence of possible effects on muscle synergies extraction. In gait, weight values for Rectus Femoris proximal and distal regions, Soleus Medialis and Lateralis and Vastus Medialis' proximal and distal end were in fact comparable and no difference stood out during tests.

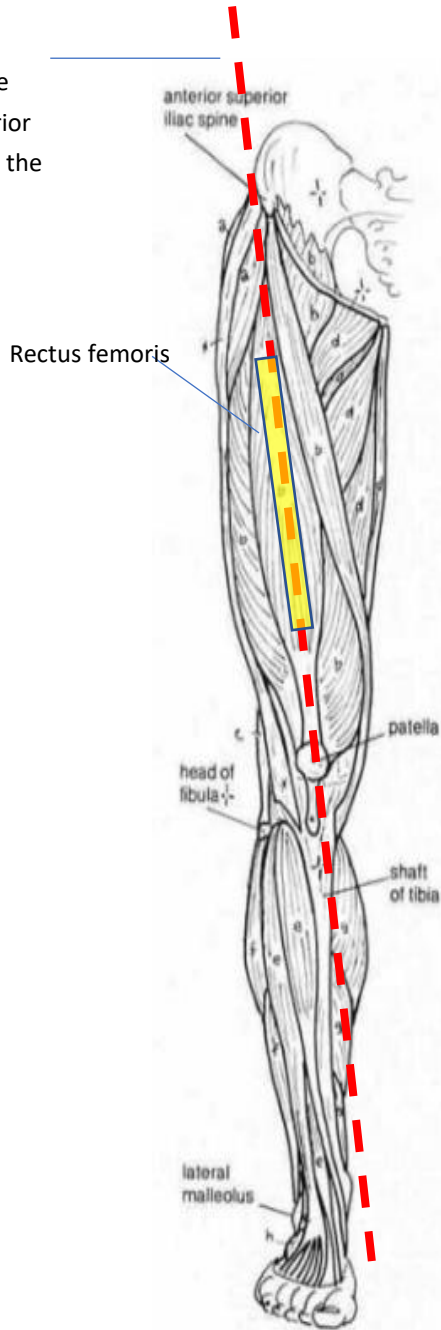
It's true, however, that in cycling muscle synergies analysis an interesting and consistent difference in muscle weights from Rectus Femoris' proximal and distal regions was found in the second synergy. This is a promising result for future evaluations, which should include a higher number of subjects and more similar conditions and set-ups to those suggested in those works which investigated different functionalities within the same muscles ^{[2][3][4][35]}.

Appendix A - anatomical pictures for each muscle with relative electrode positioning

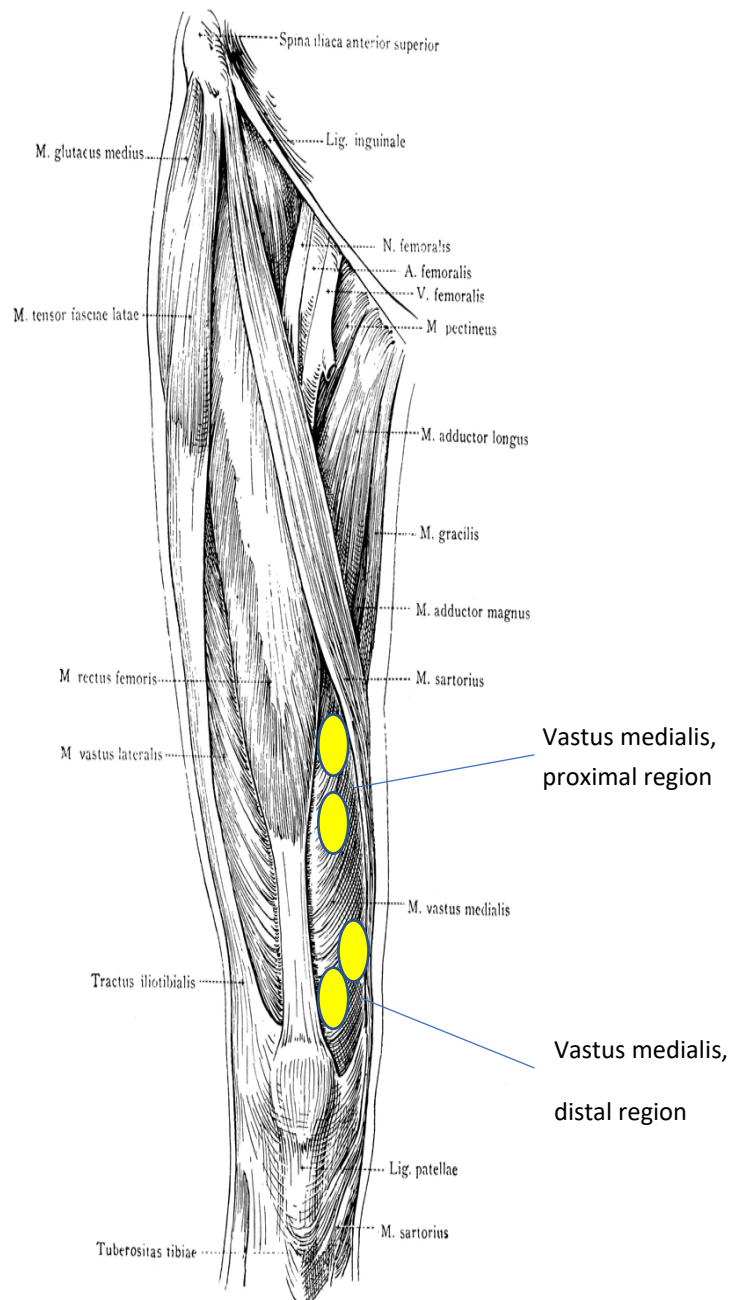
Notice that yellow shapes represent theoretical electrode locations, which must be adjusted with respect to every subject's personal anatomical conformation.

Rectus Femoris (leg frontal view)

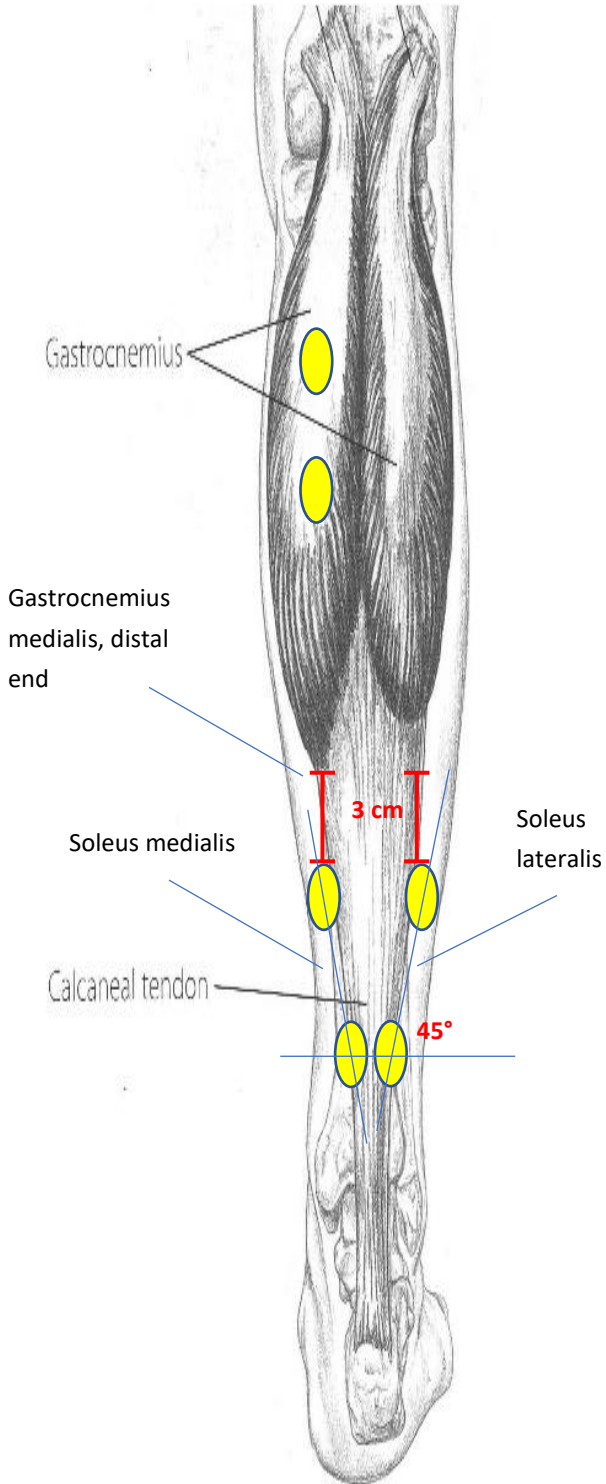
Ideal line connecting the anterior superior iliac spine and the patella



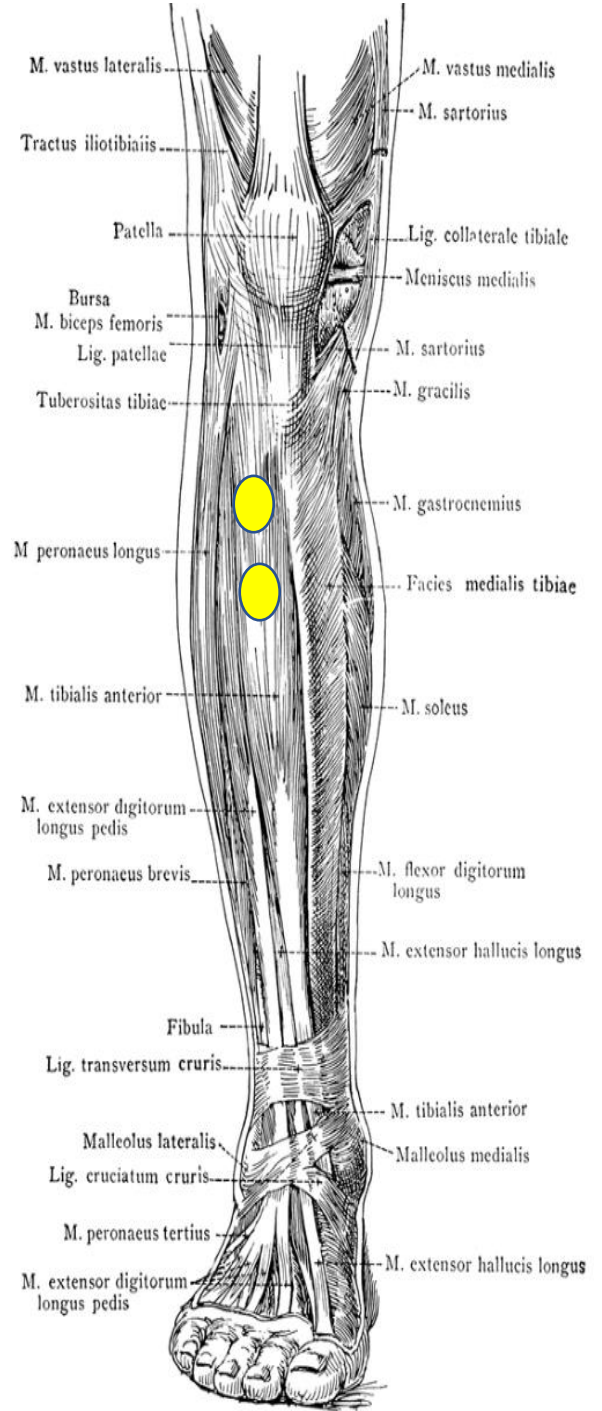
Vastus Medialis (leg frontal view, close-up on quadriceps muscles)



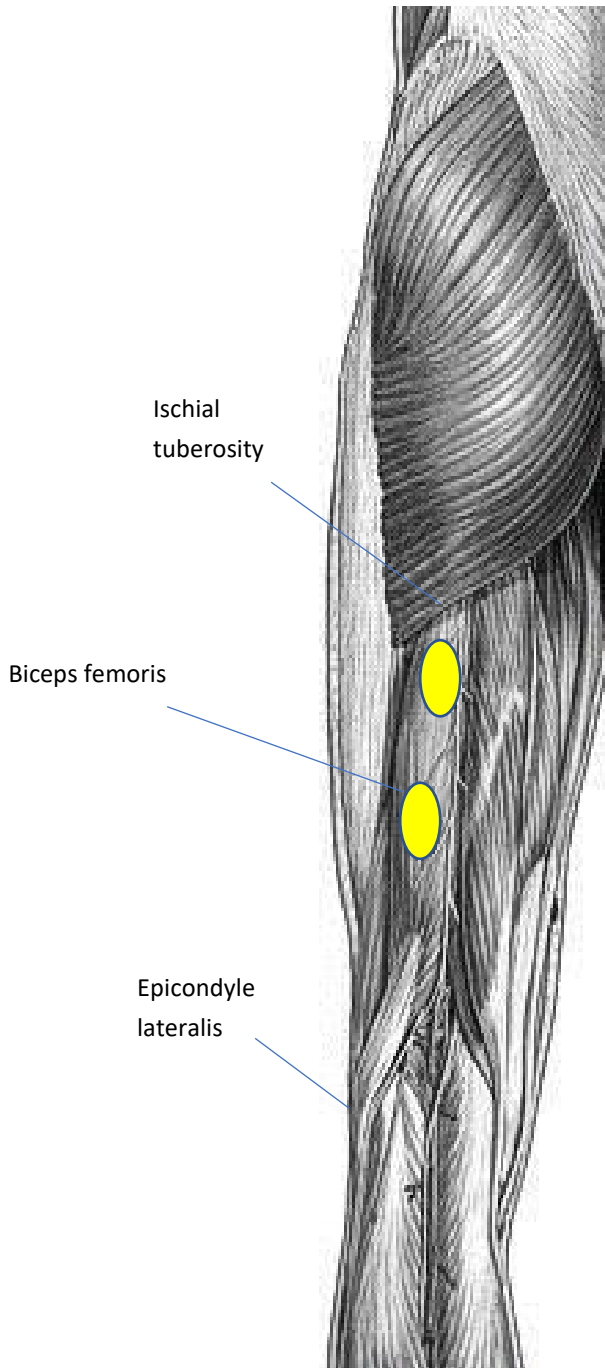
Gastrocnemius and soleus (leg rear view)



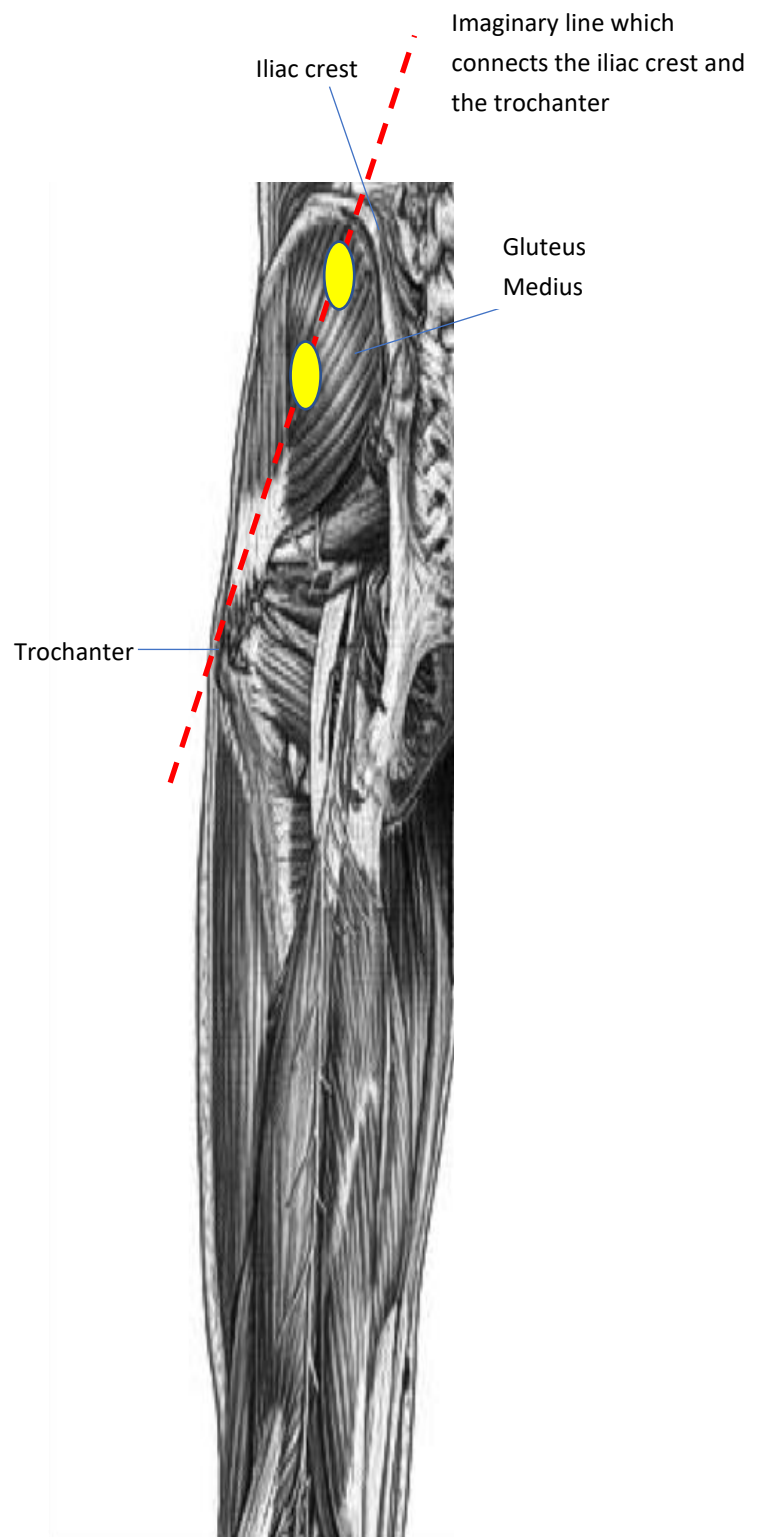
Tibialis anterior (leg frontal view)



Biceps Femoris (back view)



Gluteus Medius (back view)



Appendix B - Informed Consent

Researcher:

Subject:

Age: _____ Height (cm): _____ Weight (kg): _____

Place and date of the experiment:

OVERALL DESCRIPTION OF THE EXPERIMENTAL PROTOCOL AND GOALS

The main goal of this work is assessing the effects of electrode positioning on muscle synergies extraction. In order to simulate muscle synergies, non-invasive electromyographic signals will be detected from some lower limb muscles. Signals required from the experiment are from Rectus Femoralis, Vastus Medialis, Biceps Femoris, Gluteus Medius, Tibialis Anterior, Gastrocnemius medialis and Soleus.

Subject's skin must be clean, scrubbed and hairless as adhesive electrodes will be placed on it to detect EMG signals.

At first, every subject will be asked to walk over ground in straight line for 1 minute at self-selected speed and rest for 3 minutes. This task will be performed two times. The same task will be then repeated using a treadmill for the same amount of times.

After gait, subjects will be engaged in a 1-minute long ride on a stationary bike, at fixed resistance and pace of 40 cycles per minute. Again, this trial will be repeated three times in total.

The entire duration of the experimental protocol is around 3 hours, it will take place at LISIN (Laboratorio di Ingegneria del Sistema Neuromuscolare), Politecnico di Torino and it will be carried out by LISIN staff members.

It is also likely that subjects will be asked to sit down or lay down on a table to let a LISIN staff member check bone landmark and muscles conformation through palpation. This might be required if a first visual inspection wasn't satisfactory.

POSSIBLE RISKS

This experimental protocol is totally safe and without any danger. At the end of the experiments, subject' skin could be a little irritated after having removed the electrodes; this phenomenon might last for about an hour. Removing electrodes from skin usually causes a feeling which is similar to taking off a plaster.

Please notice that any personal information will remain confidential and won't be used or shown. Pictures of the experimental set-up will be taken only under subject's personal consent and will be added to scientific works or presentations without any physically recognizable trait.

DECLARATION OF INFORMED CONSENT

I DECLARE THAT I READ AND UNDERSTOOD EVERY PART OF THIS DOCUMENT, I RECEIVED COMPLETE ANSWERS TO MY QUESTIONS ABOUT IT AND I AM COMMITTED TO TAKE PART IN THIS STUDY.

Subject' signature:

Date:

Researcher' signature:

Date:

LISIN, Politecnico di Torino, Corso Castelfidardo 42/a, CAP 10138, Torino (TO)

Appendix C – Electrodes and skin preparation

A precise procedure must be followed step-by-step to prepare electrodes and subjects in the right way:

- Choose which detection system is suitable for the situation: arrays are perfect for parallel muscles, while matrixes are usually ideal for multipennate muscles; in this case, an 16x2 electrodes array and couples of bipolar electrodes are used;
- An adequate double-adhesive foam is to be selected to support the array: its function is to create an adhesive surface which is in contact with the skin; no foam is needed for the bipolar electrodes, which are disposable and directly placeable on the subject's skin;
- The protective film of the foam is removed to uncover the first adhesive side and the array is positioned upon it;
- Conductive paste is now spread on the whole foam, on the array side; the layer of conductive paste must be thin, yet visible and it must cover all electrodes regularly. Any excessive paste needs to be removed, since it may cause short circuit between some electrodes.
- Before positioning the array/disposable bipolar electrodes on the subject's skin, the superficial skin layer is to be removed since it may cause degradation in the electrode-skin interface, so some abrasive paste is applied to scrub the skin before positioning the electrodes. Scrubbing is taken on until the skin shows pale redness, which is a sign of cleaned skin. Any hair must be removed too.
- A suitable region for reference electrodes has to be chosen and it'd better be a visible bone end (knee, elbow, hip for example) or any other point where neuromuscular activity is virtually absent. No reference electrode is needed in the case of Due probes.

- The second adhesive layer can be now removed and the foam with the array on it can be attached to the subject's skin.
- EMG and biomechanical probes can be switched on, *bp*[®] can be activated and acquisition can start.

Bibliography

The whole introductory chapter is based on these two works:

R. Merletti, A. Botter, A. Merlo, M. A. Minetto, 2009. *Technology and instrumentation for detection and conditioning of the surface electromyographic signal: State of the art. Clinical Biomechanics* 24.

R. Merletti, P.A. Parker, 2004. *Electromyography: Physiology, Engineering and Noninvasive Applications. IEEE Press, chapter 1.*

All articles, books and works consulted throughout the realization of the other chapters are reported below:

1. **K. Watanabe, M. Kouzaki, T. Moritani**, 2012. *Region-Specific Myoelectric Manifestations of Fatigue In Human Rectus Femoris Muscle.*

2. **H. V. Cabral, L. M. de Souza, R. G. Mello, A. Gallina, L. F. de Oliveira, T. M. Vieira**, 2018. *Is the firing rate of motor units in different vastus medialis regions modulated similarly during isometric contractions? Muscle Nerve*, 57: 279-286.

3. **F. V. Dos Anjos, T. P. Pinto, M. Gazzoni and T. M. Vieira**, 2017. *The Spatial Distribution of Ankle Muscles Activity Discriminates Aged from Young Subjects during Standing. Front. Hum. Neurosci.* 11:190.

4. **K. Watanabe, M. Kouzaki, T. Moritani**, 2015. *Spatial EMG potential distribution of biceps brachii muscle during resistance training and detraining, T. Eur. J. Appl. Physiol. (2015) 115: 2661.*

5. **P. Saltiel, K. Wyler-Duda, A. d'Avella, M. C. Tresch, E. Bizzi**, 2001. *Muscle synergies encoded within the spinal cord: evidence from focal intraspinal NMDA iontophoresis in the frog. J. Neurophysiol.* 85 605–619.

6. **M. C. Tresch, E. Bizzi**, 1999. *Responses to spinal microstimulation in the chronically spinalized rat and their relationship to spinal systems activated by low threshold cutaneous stimulation. Exp. Brain Res.* 129 401–416.

7. **A. d'Avella, E. Bizzi**, 2005. *Shared and specific muscle synergies in natural motor behaviors. Proc Natl. Acad. Sci USA* 102: 3076–3081, 2005.

8. **J. Frère, F. Hug**, 2012. *Between-subject variability of muscle synergies during a complex motor skill*. *Front. Comput. Neurosci.* 6:99.
9. **A. Saito, A. Tomita, R. Ando, K. Watanabe, H. Akima**, 2018. *Muscle synergies are consistent across level and uphill treadmill running*. *Scientific Reports* volume 8, Article number: 5979 (2018).
10. **N. Dominici, Y. P. Ivanenko, G. Cappellini, A. d'Avella, V. Mondì, M. Cicchese**, et al., 2011. *Locomotor primitives in new-born babies and their development*. *Science* 334 997–999.
11. **E. Bizzi, V.C.K. Cheung**, 2013. *The neural origin of muscle synergies*. *Frontiers in computational Neuroscience* 7 (2013).
12. **V. C. K. Cheung, A. Turolla, M. Agostini, S. Silvoni, C. Bennis, P. Kasi** et al., 2012. *Muscle synergy patterns as physiological markers of motor cortical damage*. *Proc. Natl. Acad. Sci. U.S.A.* 109 14652–14656.
13. **A. Ebied, E. Kinney-Lang, L. Spyrou, J. Escudero**, 2018. *Evaluation of matrix factorization approaches for muscle synergy extraction*. *Medical Engineering & Physics*, volume 57, July 2018.
14. **D. D. Lee, S. H. Seung**, 1999. *Learning the Parts of Objects by Non-Negative Matrix Factorization*, *Nature*, November 1999. *Nature* 401, 788–791.
15. **D. Rimini, V. Agostini, M. Knaflitz**, 2017. *Intra-Subject Consistency during Locomotion: Similarity in Shared and Subject-Specific Muscle Synergies*, *Front. Hum. Neurosci.* 11:586.
16. **P. Bingyu, S. Y. X. Bin, H. Zhipei, W. Jiankang, H. Jiateng, L. Yijun, H. Zhen, Z. Zhiqiang**, 2018. *Alterations of Muscle Synergies During Voluntary Arm Reaching Movement in Subacute Stroke Survivors at Different Levels of Impairment*, *Frontiers in Computational Neuroscience*, volume 12, *Front. Comput. Neurosci.* 2018 21; 12:69. Epub. 2018 Aug 21.
17. **A. de Rugy, G. E. Loeb, T. J. Carroll**, 2013. *Are muscle synergies useful for neural control?* *Frontiers in computational neuroscience* vol. 7 19. 21 Mar. 2013.
18. **A. S. Olivera, L. Gizzi, D. Farina, U. G. Kersting**, 2014. *Motor modules of human locomotion: influence of EMG averaging, concatenation, and number of step cycles*. *Front. Hum. Neurosci.*, 23 May 2014.

19. **G. L. Cerone, A. Botter, M. Gazzoni**, 2019. *A Modular, Smart, and Wearable System for High Density sEMG Detection*, *IEEE Transactions on Biomedical Engineering*. PP. 1-1. 10.1109/TBME.2019.2904398.
20. **F. O. Barroso, D. Torricelli, J. C. Moreno, J. T., J. Gomez-Soriano, E. Bravo-Esteban, S. Piazza, C. Santos, J. L. Pons**, 2014. *Shared muscle synergies in human walking and cycling*. *J Neurophysiol* 112: 1984–1998, 2014.
21. **K. Saitou, T. Masuda, D. Michikami, R. Kojima, M. Okada**, 2001. *Innervation zones of the upper and lower limb muscles estimated by using multichannel surface EMG*. *Journal of human ergology*. 29. 35-52. 10.11183/jhe1972.29.35.
22. **A. Gallina and T. Vieira**, 2015. *Territory and fiber orientation of vastus medialis motor units: A Surface electromyography investigation*. *Muscle Nerve*, 52: 1057-1065.
23. **D. Staudenmann, I. Kingma, A. Daffertshofer, D. F. Stegeman, J. H. Van Dieën**, 2009. *Heterogeneity of muscle activation in relation to force direction: a multi-channel surface electromyography study on the triceps surae muscle*. *J. Electromyogr. Kinesiol.* 19, 882–895.
24. **H. J. Hermens, B. Freriks, R. Merletti**, 1999. *European Recommendations for Surface ElectroMyoGraphy: Results of the SENIAM Project*. Enschede, The Netherlands: Roessingh Research and Development, 1999.
25. **D. J. Clark, L. H. Ting, F. E. Zajac, R. R. Neptune, S. A. Kautz**, 2010. *Merging of healthy motor modules predicts reduced locomotor performance and muscle coordination complexity post-stroke*. *J Neurophysiol.* 2010;103(2):844–857.
26. **S.A. Kautz, M.G. Bowden, D.J. Clark, R.R. Neptune**, 2011. *Comparison of Motor Control Deficits During Treadmill and Overground Walking Poststroke*. *Neurorehabilitation and Neural Repair*, 2011; 25(8): 756-765.
27. **S. J. Lee, J. Hidler**, 2008. *Biomechanics of overground vs. treadmill walking in healthy individuals*, 2008; *Journal of Applied Physiology*; 104(3): 747-755.
28. **D. Lee, H. Seung**, 1999. *Learning the parts of objects by non-negative matrix factorization*. *Nature* 401, 788–791 (1999).

29. **G. Cappellini, R. Y. P. Ivanenko, E. Poppele, F. Lacquaniti**, 2006. *Motor patterns in human walking and running. J Neurophysiol* 95: 3426–3437, 2006.
30. **F. Hug, N. A. Turpin, A. Couturier, S. Dorel**, 2011. *Consistency of muscle synergies during pedaling across different mechanical constraints. J. Neurophysiol.* 106, 91–103.
31. **O. F. Barroso, D. Torricelli, E. Bravo-Esteban, J. Taylor, J. Gómez-Soriano, C. Santos, J. C. Moreno, J. L. Pons**, 2016. *Muscle Synergies in Cycling after Incomplete Spinal Cord Injury: Correlation with Clinical Measures of Motor Function and Spasticity. Front. Hum. Neurosci.* 2016, 9:706.
32. **C. L. Banks, M. M. Pai, T. E. McGuirk, B. J. Fregly, C. Patten**, 2017. *Methodological Choices in Muscle Synergy Analysis Impact Differentiation of Physiological Characteristics Following Stroke. Front. Comput. Neurosci.* 11:78.
33. **M. van der Krogt, L. Oudenhoven, A. I. Buizer, A. Dallmeijer, N. Dominici, J. Harlaar**, 2016. *The effect of EMG processing choices on muscle synergies before and after BoNT-A treatment in cerebral palsy. 31. Poster session presented at ESMAC 2016, Seville, Spain.*
34. **K. Watanabe, M. Kouzaki, T. Moritani**, 2012. *Task-dependent spatial distribution of neural activation pattern in human rectus femoris muscle. J. Electromyogr. Kinesiol.*, 2012, 22, 251-258.
35. **K. Watanabe, M. Kouzaki, T. Moritani**, 2014. *Regional neuromuscular regulation within human rectus femoris muscle during gait. J. Biomechanics.*, 2014, 47(14), 3502-3508.
36. **P.O. Riley, J. Dicharry, J. Franz, U. Della Croce, R. P. Wilder, D. C. Kerrigan**, 2008. *A kinematics and kinetic comparison of overground and treadmill running., Med Sci Sports Exerc.* 2008 Jun;40(6):1093-100.

Acknowledgements

All applications of multi-channel sEMG detection and algorithms realization for synergies extraction have taken place at *LISIN (Laboratory for Engineering of the Neuromuscular System)*, Politecnico di Torino. I would like to sincerely thank all students, PhDs and professors who helped and assisted me throughout the entire duration of this work, in particular Professor and LISIN director M. Gazzoni, Prof. T. Vieira Martins, Prof. A. Botter and Engr. L. G. Cerone for their patience and helpfulness. Huge thanks also go to PhDs Fabio Vieira Dos Anjos and Talita Peixoto Pinto, who have gently shared the measurements lab with me and have always been at disposal for everything I needed.

My parents Massimo and Monica, who have provided me with unconditional love and support in both my academic and sport life, deserve a special thank for every effort they have put in and every piece of advice they have given me. This whole personal journey wouldn't have been possible without them.

My sister Ilaria and I share a strong bond not only as siblings, but as trust-worthy and sincere friends: she's been next to me for my entire life and she is irreplaceable for every little thing she does.

My love Elisa shares a lot of interests and personal passions with me, from sport to games: getting along with her has been a key part of these years and her love has always been there when it counted the most. Hopefully, this will be a strong base to start building a new chapter of our lives together.

Tennis has allowed me to meet great players and friends and I'm so thankful to have learnt so much from each of them sharing courts and practices together. However, Stefano Dolce must receive a special tribute due to all the hours he has spent with me on the court. He is a humble, honest and incredibly skilful tennis coach and player, who has also become one of my best friends.

